The Global Paleomonsoon as seen through speleothem records from Asia and the Americas

Hai Cheng · Ashish Sinha · Xianfeng Wang ·
Francisco W. Cruz · R. Lawrence Edwards

Abstract The regional monsoons of the world have long been viewed as seasonal atmospheric circulation reversal—analogous to a thermally-driven land-sea breeze on a continental scale. This conventional view of monsoons is now being integrated at a global scale and accordingly, a new paradigm has emerged which considers regional monsoons to be manifestations of global-scale seasonal changes in response to overturning of atmospheric circulation in the tropics and subtropics, and henceforth, interactive components of a singular Global Monsoon (GM) system. The paleoclimate community, however, tends to view 'paleomonsoon' (PM), largely in terms of regional circulation phenomena. In the past decade, many high-quality speleothem oxygen isotope (δ^{18}O) records have been established from the Asian Monsoon and the South American Monsoon regions that primarily reflect changes in the integrated intensities of monsoons on orbital-to-decadal timescales. With the emergence of these high-resolution and absolute-dated records from both sides of the Equator, it is now possible to test a concept of the 'Global-Paleo-Monsoon' (GPM) on a wide-range of time-scales. Here we present a comprehensive synthesis of globally-distributed speleothem δ^{18}O records and highlight three aspects of the GPM that are comparable to the modern GM: (1) the GPM intensity swings on different timescales; (2) their global extent; and (3) an anti-phased inter-hemispheric relationship between the Asian and South American monsoon systems on a wide range of timescales.

Keywords Speleothem · δ^{18}O record · Global Paleomonsoon · Asian Monsoon · South American Monsoon

This paper is a contribution to the special issue on Global Monsoon Climate, a product of the Global Monsoon Working Group of the Past Global Changes (PAGES) project, coordinated by Pinxian Wang, Bin Wang, and Thorsten Kiefer.

H. Cheng (✉)
Institute of Global Environmental Change,
Xi'an Jiaotong University, Xi'an 710049, China
e-mail: cheng021@umn.edu

H. Cheng · R. L. Edwards
Department of Earth Sciences, University of Minnesota,
Minneapolis, MN 55455, USA

A. Sinha
Department of Earth Science, California State University
Dominguez Hills, Carson, CA 90747, USA

X. Wang
Earth Observatory of Singapore, Nanyang Technological
University, Nanyang Avenue 639798, Singapore

F. W. Cruz
Instituto de Geociências, Universidade de São Paulo,
Rua do Lago, 562, CEP 05508-080 São Paulo, SP, Brazil

1 Introduction

The word 'monsoon' is derived from an Arabic word '*Mausim*', which means 'season'. Although the term monsoon was originally used to describe the large-scale reversal of surface winds over the Indian Ocean during the boreal summer, in the modern parlance, it is now used to describe significant seasonal atmospheric circulation change associated with changes in wind direction and precipitation in low latitude regions. The term 'Global Monsoon' (GM) was coined to refer global-scale seasonal changes in the atmospheric circulation, particularly emphasizing the connection among major regional

monsoon systems in the tropics and subtropics on both sides of the Equator (e.g., Trenberth et al. 2000). The GM embodies a system characterized by a persistent global-scale overturning of the atmosphere that varies according to the time of year. These changes are associated with seasonal reversal in surface winds and shifts in precipitation tied to the seasonal migration of the Intertropical Convergence Zone (ITCZ) and reversal in the northern and southern hemispheric heating and temperature gradients between continent and ocean in response to the annual solar cycle (e.g., Trenberth et al. 2000; Qian et al. 2002; Wang and Ding 2006; Wang and Ding 2008).

Although the concept of the GM was proposed more than a decade ago (e.g., Trenberth et al. 2000), the paleo-climate community has yet to fully test this concept on longer timescales. In most cases, the proxy-inferred site-specific paleomonsoon (PM) variability have been viewed as one resulting from the regional monsoon variability. In 2007, a Past Global Changes (PAGES) Working Group on 'Global-Monsoon' was established in an effort to bring this holistic approach to PM research. The PAGES sponsored Global Monsoon Symposiums in 2008 and 2010 brought together paleo- and modern climatologists for in-depth discussions on the concept of the GM and its potential applicability to the 'Global-Paleo-Monsoon' (GPM) on longer timescales (Wang et al. 2009). A timely review by Wang (2009) further provides a profound analysis and description of GPM scenarios from tectonic ($\sim 10^8$–10^6 years) to millennial-centennial (10^3–10^2 years) scales.

The dominant monsoon systems in the world include the Asian–Australian, African, and the American Monsoons (e.g., Wang and Ding 2008; Zhou et al. 2008). While each of these modern regional monsoon systems has specific characteristics, all are coordinated by the annual cycle of solar radiation. In the past decade, speleothem oxygen isotope ($\delta^{18}O$) based studies have been widely used to reconstruct patterns of PM changes, most notably from Asian and South American Monsoon regions. These speleothem $\delta^{18}O$ records have proven remarkably valuable because of their high-resolution and absolute-dated features that not only allow comprehensive reconstructions of regional PM patterns but also permit robust correlations among them.

Recently, Caley et al. (2011a) using a variety of proxy records with varying chronological resolutions and uncertainties from different monsoon systems, disputes the concept of the GPM. Here we argue that a thorough test of the GPM scenario on a wide range of timescales is best accomplished through the use of well-dated and precipitation-sensitive speleothem records from various monsoon systems from both hemispheres. Accordingly, we examine a number of existing speleothem $\delta^{18}O$ records from Asia, the Americas, and the Eastern Mediterranean to highlight the major characteristics of the GPM on different time-scales and provide possible dynamical mechanisms explaining linkages among different monsoon systems.

2 Speleothem $\delta^{18}O$ records of regional monsoons

2.1 The Asian Monsoon domain

Nearly two-thirds of the global population lives under the direct influence of the seasonal rainfall associated with the Asian summer monsoon (ASM). Spring-time solar heating of the Asian continent overturns the atmosphere circulation and initiates the ASM, which transports large amounts of moisture and heat northward from northern Australia across the Indian Ocean, into India, southeastern China, and as far as northeastern China and Japan. Following the annual cycle of solar heating, during the boreal winter, cold-dry Asian winter monsoon flows from Siberia southward across eastern China, India, and the Indian Ocean, ultimately contributing to the Australian summer monsoon (An 2000).

The ASM regime includes two interactive sub-components: the East Asian summer monsoon (EASM) and the Indian summer monsoon (ISM) (Fig. 1). Although one may divide these two sub-monsoon systems geographically, it is unfeasible to clearly distinguish them mechanistically, as modern observations show that the ISM circulation and associated moisture penetrate northeastward, deep into East Asia (Figs. 1 and 2). As a result, it has been argued that a significant component of EASM precipitation (for example, in southeastern China) is derived essentially from the ISM domain (e.g., Ding 2004; Clemens et al. 2010; Pausata et al. 2011). EASM variations on a variety of timescales have been well characterized by speleothem $\delta^{18}O$ records from southeastern China, such as from Sanbao (Wang et al. 2008; Cheng et al. 2009b), Hulu (Wang et al. 2001; Cheng et al. 2006), Dongge (Yuan et al. 2004; Dykoski et al. 2005; Wang et al. 2005; Kelly et al. 2006), Wanxiang (Zhang et al. 2008) and Linzhu (Cheng et al. 2009b) Caves (Fig. 1). Variations in the ISM have been documented from speleothem records from Hoti, Qunf, Defore, and Mukalla Caves in the Arabian Peninsula (Fleitmann et al. 2003, 2007, 2011); Moomi and Dimarshim Caves in Socotra Island (Burns et al. 2003; Fleitmann et al. 2007; Shakun et al. 2007); Timta Cave in northwestern India (Sinha et al. 2005); Xiaobailong Cave in Southwestern China (Cai et al. 2011) and Tianmen Cave in the Tibetan Plateau, China (Cai et al. 2010). The aforementioned ISM records, though limited in temporal duration, sketch out major features of the PM variability in the region and together with speleothem records from the EASM domain, illustrate ASM variations on orbital-millennial-centennial-decadal time-scales and provide an important test of the GPM.
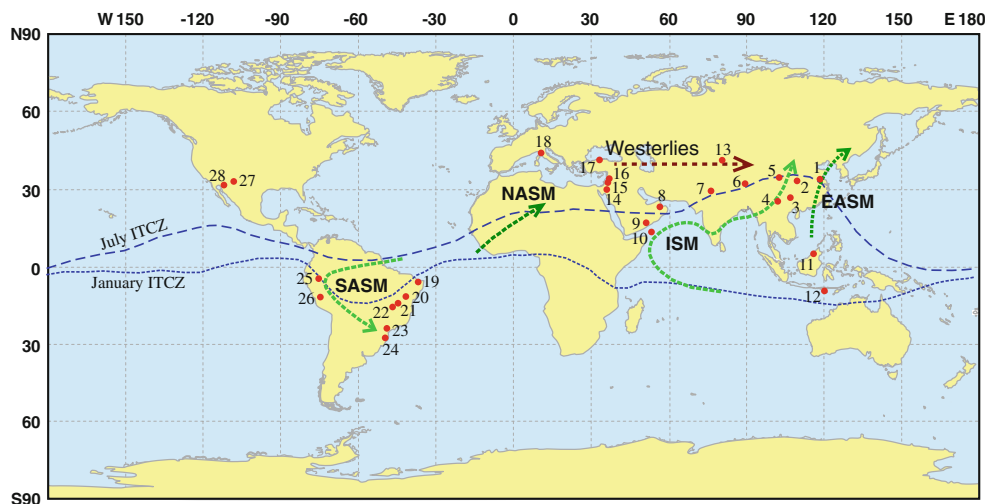
Fig. 1 Map of cave locations. *Red dots* indicate cave sites: 1-Hulu (32°30′N, 119°10′E), 2-Sanbao (31°40′N, 110°26′E), 3-Dongge (25°17′N, 108°5′E), 4-Xiaobailong (24°12′N, 103°21′E), 5-Wanxiang (33°19′N, 105°00′E), 6-Tianmen (30°55′N, 90°4′E), 7-Timta (29°50′N, 80°02′E), 8-Hoti (23°5′N, 57°21′E), 9-Qunf (17°10′ N, 54°18′ E), 10-Moomi (12°30′N, 54°E), 11-Borneo (4°N, 114°E), 12-Liang Luar (8°32′S, 120°26′E), 13-Kesang Cave (42°52′N, 81°45′E), 14-Caves in southern Israel, 15-Soreq Cave (31.45°N, 35.03°E), 16-Peqiin Cave (32.58°N, 35.19°E), 17-Sofular (41°25′N, 31°56′E,), 18-Corchia (44°2′N, 10°17′E), 19-Rio Grande do Norte (5°36′S, 37°44′W), 20-Paixão (12°39′S, 41°3′W), 21-Padre (13°13′S, 44°3′W), 22-Lapa Grande (14°25′S, 44°22′W), 23-Santana (24°32′S, 48°44′W), 24-Botuverá (27°13′S, 49°9′W), 25-Cueva del Tigre Perdido (5°56′S, 77°18′W), 26-Pacupahuain Cave (11°14′S, 75°49′W), 27-Fort Stanton Cave (33°18′N, 105°18′W), 28-Bells Cave (31°45′N, 110°45′W). *Arrows* depict wind directions of the ISM, EASM, NASM, SASM and the Westerlies. *Dashed lines* show the modern position of the ITCZ in July and January, respectively

2.2 The South American Monsoon domain

The South American summer monsoon (SASM) is a large-scale atmospheric circulation system over most of the tropical and subtropical South American continent (Zhou and Lau 1998) and exhibit many similar features of its ASM counterpart. When the SASM dominates during the austral summer season, equatorial trade winds transport moisture westward from the tropical Atlantic across the Amazon Basin to as far east as the Andes. Blocked by the high Andes mountains to the west, the warm and humid air is then forced to turn southeastward in a form of a low-level jet (LLJ) which develops deep convection over central and southeastern Brazil (Fig. 1). During the austral winter, this atmospheric circulation is weakened or even virtually comes to a halt (Zhou and Lau 1998). Speleothem $\delta^{18}O$ records from the region shed new light on the hydroclimate history of tropical and subtropical South America. The speleothem records discussed here are mainly from Rio Grande do Norte, Paixão, Padre, Santana, Botuverá, Cueva del Tigre Perdido, Lapa Grande, and Pacupahuain Caves (Fig. 1) which not only characterize SASM variations on different timescales but also describe changes in its spatial patterns (e.g., Cruz et al. 2005, 2006, 2007, 2009a, b; Wang et al. 2004, 2006, 2007a, b; van Breukelen et al. 2008; Cheng et al. 2009a; Stríkis et al. 2011; Kanner et al. 2012).

2.3 The North American Monsoon domain

The North American Monsoon prevails mainly over the southwestern US and northwestern Mexico. In the southwestern US, during boreal summer, easterly and southeasterly winds transport moisture into the area from the Gulf of Mexico and the Gulf of California. On the other hand, Pacific westerly storms during the boreal winter provide about one-half to one-third of the annual precipitation. Recently, two speleothem $\delta^{18}O$ records from southwestern US characterized the millennial scale fluctuations in precipitation history in the region over most portions of the past 60 ka (Asmerom et al. 2010; Wagner et al. 2010) (Fig. 1).

2.4 The Eastern Mediterranean domain

The modern climate in the Eastern Mediterranean region is semiarid with rainfall occurring mainly during the boreal-winter season (December–May), associated with air masses originating from the northeastern Europe and the Atlantic Ocean through the Mediterranean Sea in the west. A number of speleothem $\delta^{18}O$ records from the region have been developed mainly from Israeli caves. The long-term speleothem $\delta^{18}O$ variations in the Eastern Mediterranean climate region have been interpreted to reflect the $\delta^{18}O$ variability of the Mediterranean Sea surface water (Bar-Matthews et al. 2003). The growth of cave calcite deposits
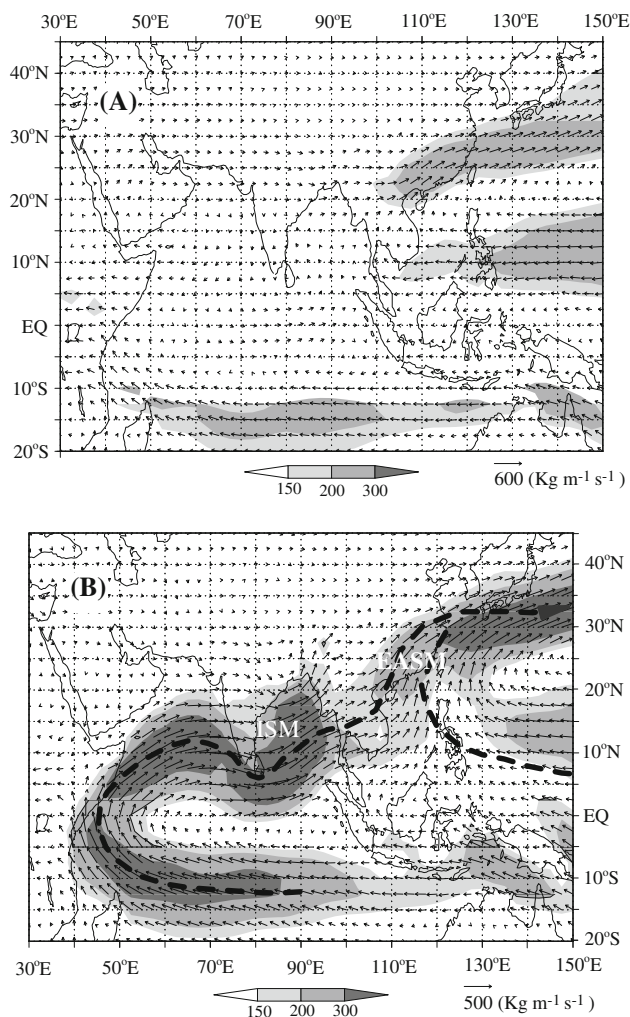
Fig. 2 Moisture transport patterns averaged for 1990–1999 (adapted from Ding 2004; Ding et al. 2004) during Pre-onset of the ASM (the 6th pentad of March-the 3rd pentad of May) (**a**) and Post-onset of the ASM (the 5th pentad of May-the 2nd pentad of July) (**b**). The strong moisture transport zone is *shaded* (in kg m^{-1} s^{-1}). Atmospheric circulation and moisture transport patterns are entirely different between pre- and post-onset of the ASM

in southern Israel appears to have occurred at the times of the strongest North African summer monsoon (NASM) (Vaks et al. 2006, 2007, 2010; Waldmann et al. 2010).

3 Speleothem δ^{18}O proxy

Speleothem calcite δ^{18}O has been widely used as a PM proxy. Although the speleothem δ^{18}O signatures can be influenced by numerous and complex factors (e.g., Fairchild et al. 2006; Lachniet 2009), robust replications among speleothem δ^{18}O records on orbital-centennial timescales from different caves in ASM and SASM regions demonstrate that these speleothems grew under conditions

close to isotopic equilibrium, and therefore their δ^{18}O records mainly represent changes in precipitation δ^{18}O values with regional extent (e.g., Cheng et al. 2006). However, the climatic interpretation of δ^{18}O records remains a subject of considerable debate, particularly in the EASM domain (e.g., Maher 2008; Dayem et al. 2010; Clemens et al. 2010; Pausata et al. 2011; Caley et al. 2011b).

In the ISM domain, precipitation δ^{18}O changes have generally been interpreted to primarily indicate variations in local rainfall amount (e.g., Burns et al. 1998, 2001, 2003; Sinha et al. 2005, 2011; Shakun et al. 2007) and this interpretation is supported by recent climate modeling studies (e.g., Vuille and Werner 2005; LeGrande and Schmidt 2009; Pausata et al. 2011). However, this explanation may not be applicable in the EASM domain. In the EASM domain, the onset of summer monsoon rainfall occurs in late May in the South China Sea and southeastern coastal areas of China, with monsoon rainfall advancing to central-eastern China by June and eventually reaching northern-northeastern China in July. During this seasonal change in precipitation, the land-sea temperature contrast increases progressively, driving stronger and larger atmospheric circulation, thus, transporting more moisture from distal ocean sources into China (Fig. 2). As a larger fraction of water vapor is removed during the transfer trajectory from more distal water sources, δ^{18}O values in precipitation become progressively lower (e.g., Yuan et al. 2004) and reach the minima during July–August (Fig. 3), coinciding with the maxima in the land-sea temperature contrast. During autumn, the δ^{18}O value becomes progressively higher with the retreat of the summer monsoon (Fig. 3). The winter (December–February) precipitation in eastern China however, shows a relatively large δ^{18}O variation from low δ^{18}O values in the north to high values in the south (Fig. 3), possibly in response to contrasting winter temperatures. In general, the aforementioned observations demonstrate that the seasonal δ^{18}O precipitation cycle correlates inversely with the summer monsoon intensity and/or the distance of moisture sources, except the lower δ^{18}O values associated with winter precipitation in North China. The latter, however, is less important because of its small contribution to the weighted mean annual precipitation in the area.

The seasonal cycle of EASM precipitation δ^{18}O can serve as an analogue for interpreting δ^{18}O variations in the speleothem records. When the Northern Hemisphere summer insolation (NHSI) is high on precessional scale, the summer (winter) insolation becomes higher (lower), while the spring–autumn insolation remains approximately the same (Berger 1978). As a result, it is plausible that both summer and winter monsoons become more intense. However, the summer monsoon enhancement may play a
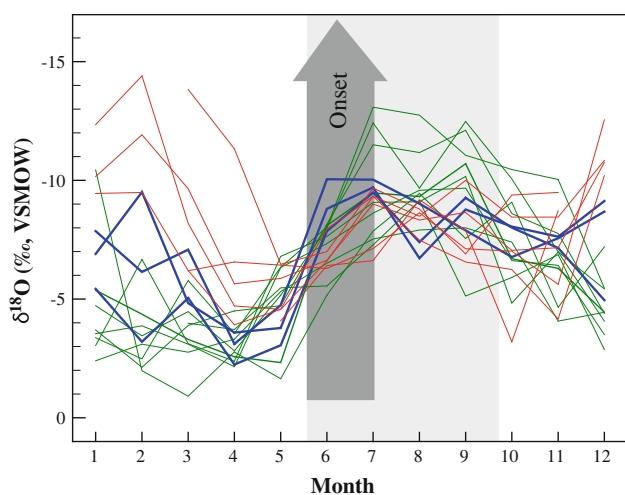
Fig. 3 Weighted monthly $\delta^{18}O$ values of precipitation obtained from meteorological observatories in eastern China (data from IAEA, accessible at: http://isohis.iaea.org). *Green curves* are from southern China (approximate 30–20°N, i.e., Hong Kong, Guangzhou, Chengdu, Guilin, Guiyang, Changsha, Haikou, Kunming, Liuzhou and Zunyi observatories). *Blue* from central eastern China (approximate 30–35°N, i.e., Nanjing, Wuhan and zhengzhou observatories), and *red* from northern China (approximate 35–40°N, i.e., Shijiazhuang, Yantai, Tianjing, Xi'an, and Taiyuan observatories). The wide *vertical arrow* indicates the onset of the summer monsoon in May at China's southeast coast, June in central eastern China and July in northern China. The *vertical grey bar* illustrates approximate time period of the summer monsoon. The summer monsoon precipitation is characterized by distinctly lower $\delta^{18}O$ than precipitation during the rest of the year. The altitude effect may have some bearing on the $\delta^{18}O$ values for the high altitude sites (e.g., Kunming). It also appears that the atmospheric temperature effect may affect the winter $\delta^{18}O$ values, because these values display a decrease trend from southern to northern China, possibly linked to the winter temperature decrease northward

more important role in modulating the mean annual $\delta^{18}O$ values in precipitation (and by extension, $\delta^{18}O$ values in speleothem) because increase in the summer insolation would lead to an overall higher summer monsoon rainfall whereas decrease in winter insolation would lead to stronger winter monsoon circulation or colder-drier conditions during winter. The speleothem $\delta^{18}O$ variance on precession cycles has, thus, been explained by a change in the ratio of the amount of summer (lower $\delta^{18}O$) to non-summer precipitation (higher $\delta^{18}O$) (Wang et al. 2001).

In eastern China, amount of local precipitation could be decoupled, to some extent, from the EASM intensity. For instance, strong summer monsoon in July–August may drive more frontal rainfall up to northern China and less in central-eastern China than in June. Modern meteorological observations on interannual-scale also show that the stronger EASM can penetrate farther into North China and bring more frontal rainfall into the region and, conversely, a weaker EASM may deliver more rainfall in central-

eastern China and less up to the north (Ding 1992). A recent simulation study shows that Holocene precipitation $\delta^{18}O$ values correlate well with summer monsoon rainfall amount in the ISM domain, but not in the EASM domain, and instead, the EASM precipitation $\delta^{18}O$ indicates the mean state of monsoon intensity or integrated summer water vapor transported into the EASM region (LeGrande and Schmidt 2009). On millennial timescale, simulation study also suggests a possible scenario that excursions of the precipitation $\delta^{18}O$ depletion (enrichment) may mainly reflect strong (weak) ASM events as a whole, rather than amount of local rainfall at an individual site in southeastern China (Pausata et al. 2011). Based on aforementioned observations, it is apparent that variations in the $\delta^{18}O$ of EASM precipitation indicate a mean state of summer monsoon intensity or integrated moisture transport rather than amount of local precipitations (Johnson and Ingram 2004; Cheng et al. 2006).

In the SASM domain, speleothem $\delta^{18}O$ records are also tightly linked to the SASM intensity (e.g., Wang et al. 2006; van Breukelen et al. 2008; Cruz et al. 2005, 2007, 2009b; Kanner et al. 2012). In southeastern Brazil, for instance, precipitation $\delta^{18}O$ has a significant negative correlation with the SASM intensity as indicated by both instrumental data and Atmospheric General Circulation Model simulations (e.g., Vuille and Werner 2005; Lee et al. 2009). There are two moisture sources that contribute to rainfalls in the region. The LLJ transports moisture eastwardly with lower $\delta^{18}O$ value due to its long trajectory (Hoffmann 2003), and the water vapor from nearby Atlantic is characterized by distinctly higher $\delta^{18}O$ (Fig. 1). As a result, the speleothem $\delta^{18}O$ variations mainly represent the change in ratio between the precipitation from the two sources (Cruz et al. 2005; Wang et al. 2006). Broadly, an enhanced SASM is associated with a stronger LLJ, hence, transporting more moisture into downstream southeastern Brazil (Liebmann et al. 2004), resulting in the lower $\delta^{18}O$ of precipitation (Cruz et al. 2006; Wang et al. 2006). On the other hand, the influence of moisture from local Atlantic source is less important on the $\delta^{18}O$ variability (Wang et al. 2006; Cruz et al. 2007). Thus, cave $\delta^{18}O$ values in the region primarily indicate the strength of the LLJ along the moisture trajectory from the Amazon Basin to southeastern Brazil (i.e., the intensity of the SASM) with lower (higher) calcite $\delta^{18}O$ in speleothem records indicating an intensified (weakened) SASM with a more (less) Amazon moisture contribution.

In the North American Monsoon region, the speleothem $\delta^{18}O$ records mainly document the change in the winter (low $\delta^{18}O$)/summer (high $\delta^{18}O$) precipitation ratio or the amount of winter precipitation which is characterized by relatively depleted $\delta^{18}O$ (Asmerom et al. 2010; Wagner et al. 2010).

4 Correlations among speleothem records

4.1 Orbital timescales

The EASM $\delta^{18}O$ record shows a broadly sinusoidal pattern with a dominant cycle of ~ 23-ka that closely follows the NHSI on precessional timescale (Yuan et al. 2004; Wang et al. 2008; Cheng et al. 2009b). Spectral analysis shows no significant phase difference between mid-July insolation and the mean EASM $\delta^{18}O$ signal (Wang et al. 2008). Recently, two hypotheses were proposed to explain the observation that the EASM follows the mid-July NHSI. (1) The first hypothesis (Wang et al. 2008) is based on the analogy that in the EASM domain, seasonal precipitation $\delta^{18}O$ reaches the minima around mid-July (Fig. 3)—when the land-sea temperature contrast becomes largest and the summer monsoon is strongest (Fig. 3). (2) EASM speleothem $\delta^{18}O$ records show an apparent phase lag of 30° (or ~ 2–3 ka) to the mid-June NHSI and this lag (but in phase with the mid-July insolation) has been attributed to the influence of high-latitude millennial-scale abrupt climate events on the EASM, which presumably delayed the monsoon response to the rising NHSI (Ziegler et al. 2010).

Although the two hypotheses are different in details, both emphasize variations in insolation as a major driving force of the EASM. Unfortunately, the speleothem records from the ISM domain are rather discontinuous on orbital timescale without a sufficient temporal coverage or resolution to fully test the insolation hypothesis. Nevertheless, existing speleothem $\delta^{18}O$ records from Qunf Cave in southern Oman (Fleitmann et al. 2003) and Timta Cave in northwestern India (Sinha et al. 2005) indeed demonstrate that variations in the ISM occurred in concert with the EASM at least over the past 15 ka (Fig. 4). The possible synchronicity between the EASM and ISM on orbital timescales is also supported by a recent speleothem record from Tianmen Cave, Tibet- a region within the ISM domain (Cai et al. 2010). The Tianmen record shows that the ISM variability during portions of the Marine Isotope Stage (MIS) 5 (mainly 5a, 5c, and 5e) is also broadly similar to Chinese EASM records (Fig. 5).

A number of speleothem $\delta^{18}O$ records from tropical-subtropical South America have demonstrated that variations in the SASM track changes in Southern Hemisphere summer insolation on orbital timescale (Cruz et al. 2005, 2007; Wang et al. 2007a) and thus, exhibit an interhemispheric anti-phased relationship with ASM records at precession bands (Fig. 6). This is because Earth's orbital precession affects the seasonal distribution of solar radiation resulting in precessional increase in northern tropical-subtropical summer insolation which is balanced by decreases in southern tropical-subtropical summer insolation and vice versa. The sea-saw oscillations in solar
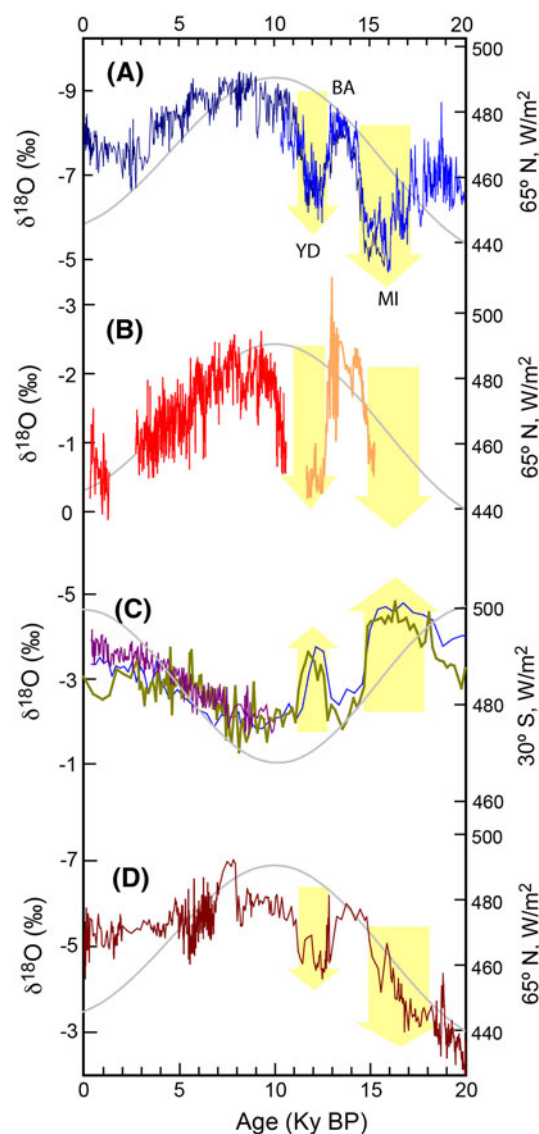
Fig. 4 Cave $\delta^{18}O$ records over the past 20 ka from EASM, ISM, SASM and Eastern Mediterranean regions. **a** EASM records from Hulu (*blue*) and Dongge (*dark blue*) Caves (Wang et al. 2001; Dykoski et al. 2005). **b** ISM records from Qunf (*red*) and Timta (*orange*, relative scale) Caves (Fleitmann et al. 2003; Sinha et al. 2005). **c** SASM records from Botuverá Cave (Cruz et al. 2005; Wang et al. 2006, 2007a). *Different colors* denote different stalagmites. **d** The Eastern mediterranean record from Soreq Cave (Bar-Matthews et al. 2003). Summer insolation (*grey curves*) at 65°N (in **a**, **b** and **d**) and 30°S (in **c**) were plotted for comparison (Berger 1978)

radiation, alternating between tropics-subtropics of two hemispheres, can thus explain the anti-phased relationship between the ASM and SASM, because the insolation forcing intensifies summer monsoon intensity due to enhanced land-sea thermal contrast (e.g., Kutzbach 1981; Kutzbach et al. 2008). Similar interhemispheric anti-phased relationship had also been noted in the African Monsoon domain. For example, South African Monsoon variations reconstructed from the Pretoria Saltpan
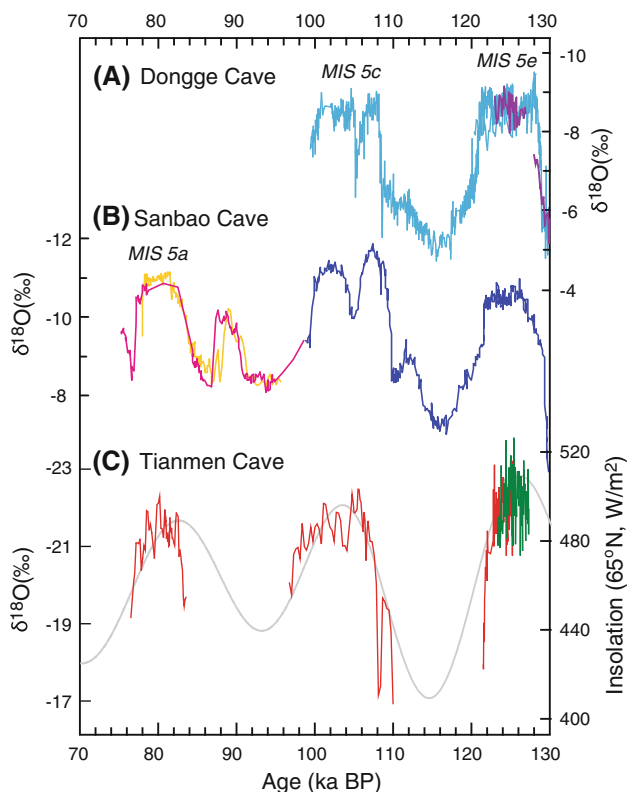
Fig. 5 Comparison between the ISM and EASM $\delta^{18}O$ records over the Marine Isotope Stage (MIS) 5 (adapted from Cai et al. 2010). **a** Hulu and Dongge records (Cheng et al. 2006; Kelly et al. 2006). **b** The Sanbao record (Wang et al. 2008). **c** The Tianmen record (Cai et al. 2010). *Different colors* denote different stalagmites. Summer insolation at 65°N (*grey*) was plotted for comparison (Berger 1978)

sedimentary record, South Africa (~ 25.5°S) (Partridge et al. 1997) and the NASM index based on fossil faunal assemblage variations in deep-sea sediment core RC24-07 (20°N) (McIntyre et al. 1989), track southern and northern tropical-subtropical summer insolation changes, respectively, during the late Pleistocene.

In the eastern Mediterranean region, a composite $\delta^{18}O$ record for the last 250 ka from Soreq and Peqiin Caves, Israel is characterized by precessional variations that are superimposed on strong 100-ka cycles (Bar-Matthews et al. 2003). The rainfall in this region is derived mainly from the adjacent Eastern Mediterranean Sea and, thus, the Soreq and Peqiin $\delta^{18}O$ records broadly follow variations in the $\delta^{18}O$ of the sea surface water, the latter being inferred from the marine *Globigerinoides ruber* $\delta^{18}O$ record (e.g., Fontugne and Calvert 1992). The $\delta^{18}O$ of surface water of the Mediterranean Sea is primarily controlled by river discharge, local precipitation/evaporation, and exchanges of the Mediterranean Sea water with the Atlantic Ocean through the Strait of Gibraltar, and with the Black Sea through the Dardanelles/Bosporus Straits (Badertscher et al. 2011).

Because the Atlantic seawater $\delta^{18}O$ variance is dominated by the 100-ka cyclicity (e.g., Lisiecki and Raymo 2005), the water exchange between the Mediterranean Sea and Atlantic waters (except during the periods characterized by formation of Mediterranean sapropels) presumably modulated the $\delta^{18}O$ variability of the Eastern Mediterranean Sea surface water on a 100-ka periodicity (e.g., Arz et al. 2003; Tzedakis 2007; Rohling et al. 2009; Göktürk et al. 2011) and thus, by extension, the $\delta^{18}O$ variations in Soreq and Peqiin records. On the other hand, the Eastern Mediterranean Sea also receives large quantity of freshwater discharge from the northern Africa rivers (e.g., the Nile River). The precession cyclicity of the NASM, exerted on the fluctuations in freshwater discharge, can be imprinted in marine sediment and speleothem records in the region as well (e.g., Rossignol-Strick et al. 1982; Rossignol-Strick 1983; Pokras and Mix 1987; Weldeab et al. 2007; Ruddiman 2008; Ziegler et al. 2010). Recently, a remarkable correlation has been established between the Eastern Mediterranean ODP 968 color reflectance and ASM records (Ziegler et al. 2010), further suggesting an in-phased response of ASM and NASM systems to external forcing (Fig. 6).

The speleothem records from Soreq Cave, Israel (Bar-Matthews et al. 2003) and Antro del Corchia, Italy (Drysdale et al. 2009) are characterized by a gradual decrease in $\delta^{18}O$ values during a Weak Monsoon Interval characterized in the EASM record around Termination II when the sea level was presumably rising (Cheng et al. 2009b) (Fig. 7). Following the gradual decreasing trend is an abrupt decrease in $\delta^{18}O$ at ~ 129 ka in both Israeli and Italian records, which is correlated, within dating errors, with an abrupt increase in both ASM (Cheng et al. 2009b) and NASM (Weldeab et al. 2007) (Fig. 7) intensities. A plausible mechanism may involve a gradual rise in sea level from the continental ice meltdown followed by an abrupt increase of the Nile River discharge due to abrupt intensification of the NASM. This hypothesis is consistent with the observation that while the magnitude of $\delta^{18}O$ change in both Israeli and Italian cave records, corresponding to the gradual rise of the sea level, is similar, the abrupt decline in $\delta^{18}O$ values at Israeli cave sites is much larger (more than 2 ‰) than the Italian site (slightly less than 1 ‰) (Fig. 7). The disparity in the $\delta^{18}O$ amplitude likely stems from the fact that the Israeli site being in a close proximity with the Eastern Mediterranean was more sensitive to changes in the Nile River discharge (Fig. 1).

Today, the Saharan-Arabian Desert is the largest and the most arid region in the world. However, this modern hyper-arid region appears to have many humid periods in its Quaternary climate history, when the summer monsoon was stronger during times when the NHSI was much higher than today, leading to formations of lakes and rivers (e.g.,
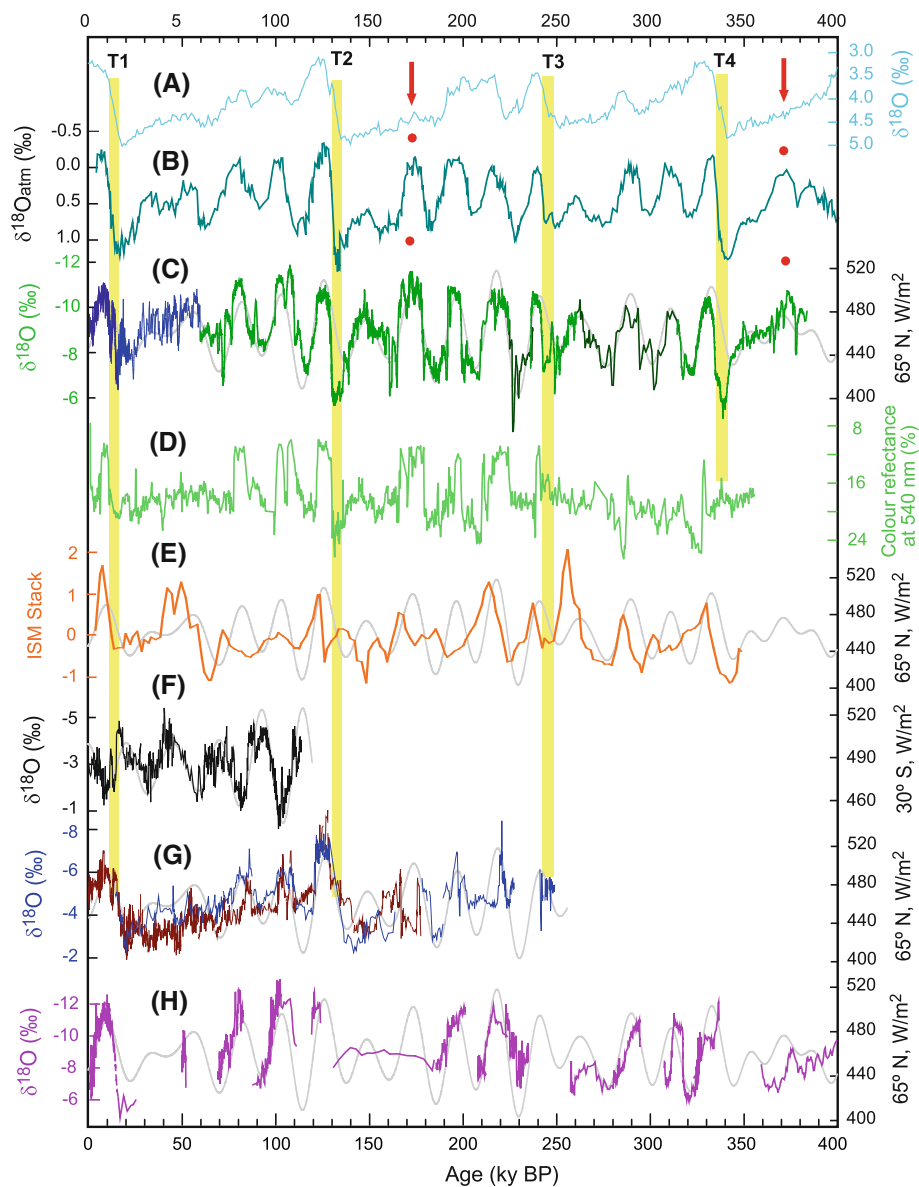
Fig. 6 Comparison among the benthic, atmospheric and speleothem $\delta^{18}O$ records, and marine records. **a** The stacked benthic $\delta^{18}O$ record (Lisiecki and Raymo 2005). **b** The atmospheric $\delta^{18}O$ record from Vostok ice core, Antarctica (Suwa and Bender 2008). **c** EASM records are composited from records of Dongge (*dark blue*), Hulu (*blue*), Sanbao (*green*) and Linzhu (*black*) Caves (Wang et al. 2001; Dykoski et al. 2005; Wang et al. 2008; Cheng et al. 2009b). For comparison, the Hulu and Dongge $\delta^{18}O$ records are plotted 1.6 % more negative to account for their higher values than Sanbao cave. **d** The Eastern Mediterranean ODP 968 color reflectance record (540 nm, %) (Ziegler et al. 2010). **e** The stacked marine ISM record (Clemens and Prell 2003). **f** The SASM record from Botuverá Cave (Cruz et al. 2005). **g** The Eastern Mediterranean record from Soreq (*brown*) and Peqiin (*blue*) Caves (Bar-Matthews et al. 2003). **h** The Kesang Cave record

from the Westerlies region. The *vertical yellow bars* depict the Terminations (T-I to T-IV, Cheng et al. 2009b). *Red arrows* show strong ASM events during glacial times as documented by terrestrial mollusk records from the Chinese Loess Plateau (Rousseau et al. 2009) and *red dots* depict their possible correlations to the atmospheric and ASM $\delta^{18}O$ records. Summer insolation (mid-July, grey curves) at 65°N (in **c**, **e**, **g** and **h**) and 30°S (mid-January, in **f**) (Berger 1978) were plotted for comparison. While the EASM record (**c**) broadly tracks the mid-July insolation change at 65°N and proves its significant similarity to the atmospheric $\delta^{18}O$ record (**b**), the marine ISM from the Arabian Sea (**e**) appears to lag to the same insolation change by ∼8 ka at precession bands. The remarkable similarity between the Eastern Mediterranean ODP 968 (**d**) and the ASM (**c**) records demonstrates a close link between the NASM and ASM

Szabo et al. 1995; Crombie et al. 1997). Similarly, intervals of enhanced speleothem formation in the Arabian Peninsula (e.g., Hoti Cave, northern Oman, Burns et al. 1998, 2001; Fleitmann et al. 2011, Mukalla Cave, southern

Yemen Fleitmann et al. 2011) and in the Negev desert, Israel (Vaks et al. 2006, 2007, 2010) indicate episodes of wide-spread humid conditions that can be linked to intensifications of the ISM (Burns et al. 1998, 2001; Fleitmann
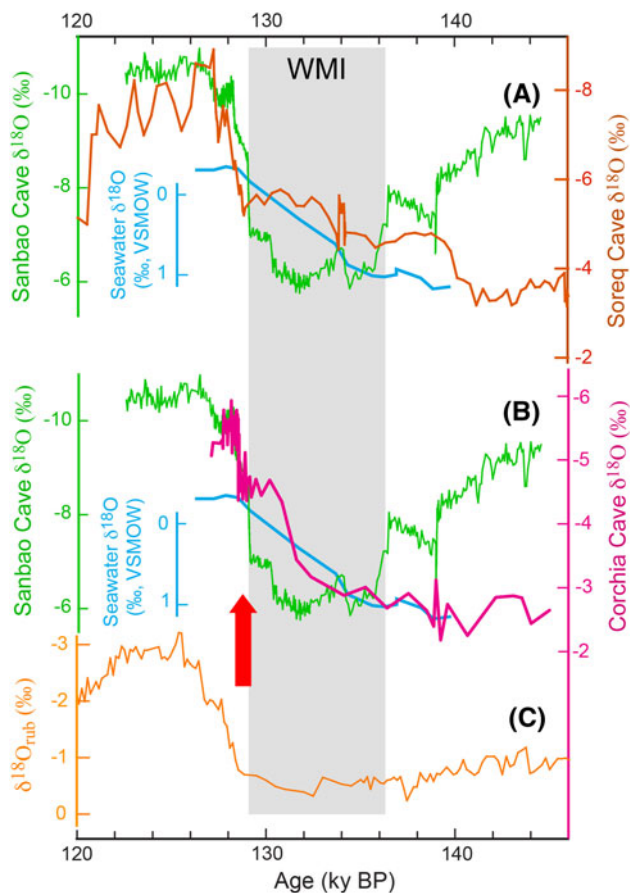
Fig. 7 Monsoon records around Termination-II. **a** *Three curves* show the Sanbao $\delta^{18}O$ record (*green*) (Wang et al. 2008), the Soreq $\delta^{18}O$ record (*brown*) (Bar-Matthews et al. 2003) and the inferred sea level (*blue*) (Cheng et al. 2009b), respectively. **b** The *green* and *blue curves* are as same as those in (**a**). The *purple cure* is the Corchia $\delta^{18}O$ record (Drysdale et al. 2009). **c** The NASM proxy record: the $\delta^{18}O$ record of planktonic foraminifer *Globigerinoides ruber* in a marine sediment core from the Gulf of Guinea (Weldeab et al. 2007). The *grey bar* denotes the Weak Monsoon Interval (WMI) recorded in ASM records (Cheng et al. 2006, 2009b). The *red arrow* indicates a synchronous jump among the ASM, NASM and $\delta^{18}O$ in Mediterranean cave records

et al. 2011) and perhaps the NASM (Waldmann et al. 2010; Battisti et al. 2012) during times of high NHSI, including MIS 1, 5.1, 5.3, 5.5, 7.1, and 9. In contrast, speleothem formation in these areas was virtually absent during glacial periods (Burns et al. 2001; Vaks et al. 2010; Fleitmann et al. 2011), implying significantly weak summer monsoon associated with glacial periods. Recently, a speleothem record from Kesang Cave in western China documents a precipitation history over the past 500 ka in the current semiarid-arid Westerlies region (Cheng et al. 2012a). The Kesang record also shows a precession rhythm that is possibly linked to incursions of ASM rainfall during the insolation peaks when the ASM was much stronger than at the present time (Fig. 6).

In summary, the aforementioned orbital-scale changes in monsoons are dominated by variation between two modes with low (high) $\delta^{18}O$ values corresponding to strong (weak) PM state. These patterns of PM variations are primarily related to summer insolation changes and, to some extent, the ice volume and possibly other factors as well. The transitions between the two modes were however, generally abrupt or non-linear in comparison to insolation forcing, possibly related to abrupt climate events at high northern latitudes (Cheng et al. 2009b; Ziegler et al. 2010) and/or due to some threshold mechanisms, such as the atmospheric humidity level over oceans around the monsoon regions and its feedbacks (Levermann et al. 2009; Schewe et al. 2011).

4.2 Millennial-centennial timescales

The ASM $\delta^{18}O$ records, most notably from China, contain prominent millennial-length events, including all the counterpart events recorded in Greenland ice core records, such as the Younger Dryas (YD), Dansgaard-Oeschger (D/O), and Heinrich (H) events (e.g., Wang et al. 2001, 2008; Ma et al. 2012). The so-called 'Chinese interstadials' (CIS) nomenclature has been introduced to indicate strong ASM events recorded in speleothem records (Cheng et al. 2006) that correlate with the D/O events during the last glacial period in Greenland ice cores. The complete series of CIS events are similar between the last and penultimate glacial periods in terms of the variability in their frequency and duration, indicating an ice volume effect on their characteristics and pacing (Cheng et al. 2006; Wang et al. 2008). The millennial events in ASM records (e.g., Wang et al. 2001, 2008; Burns et al. 2003; Cheng et al. 2006; Cai et al. 2006; Shakun et al. 2007) exhibit negative correlation with $\delta^{18}O$ records from the SASM region including both equatorial and subtropical areas (Cruz et al. 2005, 2009a, b; Wang et al. 2004; 2007a, b; Cheng et al. 2012b; Kanner et al. 2012) (Fig. 8). As noted in earlier studies, this low-latitude interhemispheric precipitation see-saw pattern is likely related to shifts in positions of the ITCZ and associated asymmetry in Hadley circulation in two hemispheres, perhaps ultimately triggered by changes in deep water formation in the North Atlantic Ocean (e.g., Lindzen and Hou 1988; Clement et al. 2004; Wang et al. 2006, 2007a b). Model simulations show that large meltwater discharge into the North Atlantic can substantially weaken the Atlantic Meridional Overturning Circulation (AMOC), resulting in increasing sea ice coverage in the northern high latitudes and meridional Atlantic sea surface temperature (SST) gradients. This, in turn, can induce significant responses in the tropics-subtropics (e.g., Chiang et al. 2003; Chiang and Bitz 2005; Zhang and Delworth 2005), resulting in a southward ITCZ shift and subsequently an
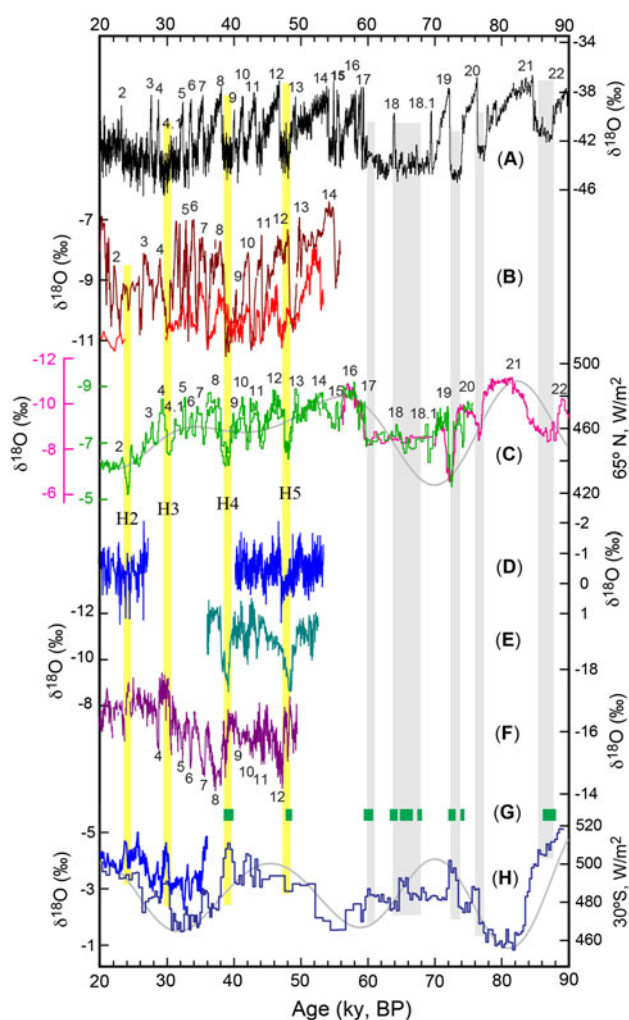
Fig. 8 Correlations among millennial events in ASM, SASM and North American Monsoon records. **a** The Greenland ice core $\delta^{18}O$ record (NGRIP, Svensson et al. 2008). **b** Speleothem records from southwestern North America: the Fort Stanton cave record (*brown*, Asmerom et al. 2010) and Bells Cave record (*red*, Wagner et al. 2010). **c** The EASM record is compiled using the Hulu (*green*, Wang et al. 2001) and Sanbao (*purple*, Wang et al. 2008) records. **d** The ISM record from Moomi Cave (Burns et al. 2003; Shakun et al. 2007). **e** The ISM record from Xiaobailong Cave (Cai et al. 2006). **f** The SASM record from Pacupahuain Cave (Kanner et al. 2012). **g** Northeastern Brazil speleothem growth (*wet*) periods (*green*) (Wang et al. 2004). **h** The SASM record from Botuverá records (*blue* (Wang et al. 2006) and *dark blue* (Wang et al. 2007a)). *Numbers indicate* Greenland Interstadials. *Vertical yellow bars* denote H events (H2–H5) and *grey bars* indicate correlations among northeastern Brazil wet periods, strong SASM events and cold Greenland-weak ASM events. Summer insolation (*grey curves*) at 65°N (in **c**) and 30°S (in **g**) (Berger 1978) were plotted for comparison

alteration of the Hadley circulation (Lindzen and Hou 1988). Such modification produces intensified uplift of moist air in the southern low latitudes but strong subsidence in the north (Lindzen and Hou 1988; Clement and Peterson 2008). As a result, the ASM is weakened while the SASM intensifies and vice versa. Indeed, similar to

their Greenland counterparts, millennial paleomonsoon events in ASM and SASM records oscillate between two states along orbital long-term trend, demonstrating a causal linkage and their interhemisphere extent.

In addition, speleothem $\delta^{18}O$ records from southwestern North America (Asmerom et al. 2010; Wagner et al. 2010) are characterized by a series of millennial events during the last glacial period (Fig. 8). When the cold events documented in Greenland ice cores occurred, the polar jet stream shifted southward, modulating the position of the winter storm tracks and winter precipitation (with distinctly lower $\delta^{18}O$ values) increased in the region (Asmerom et al. 2010). The millennial scale events in southwestern North America, both in terms of changes in precipitation $\delta^{18}O$ and amount, are anti-phased with their counterparts in the ASM domain and in-phased with those in the SASM domain (Fig. 8).

One of the most prominent and widespread abrupt climate events during the Holocene is the 8.2 ka event (Alley et al. 1997; Cheng et al. 2009a). The timing and structure of the 8.2 ka event has been well documented in ASM records (i.e., Hoti and Qunf records, Oman and the Dongge record, China) and SASM records (i.e., the Paixão, Padre and Lapa Grande records) (Wang et al. 2006; Cheng et al. 2009a; Stríkis et al. 2011). Similar to other millennial-scale climate events, the 8.2 ka event manifests as a weak (strong) monsoon event in the ASM (SASM) records. Interestingly, the magnitude of $\delta^{18}O$ excursion in the SASM records is much larger ($\sim$2.5 ‰) than that in the ASM records ($\leq$1 ‰) and tracks Greenland records closely in terms of structure (Cheng et al. 2009a). This observation is consistent with a North Atlantic origin of the event and a tight link between the Atlantic sector of the ITCZ and the North Atlantic climate (Wang et al. 2007a, b). Another notable centennial-scale event is the Little Ice Age (LIA) in human cultural history. The apparent weak ASM during the LIA (Zhang et al. 2008) coincides with the strong SASM at the same time period (Reuter et al. 2009). Furthermore, as Cheng et al. (2010) pointed out, a strong ASM period during the Chinese Northern Song Dynasty coincided with dry conditions that Tiwanaku endured in South America, which disrupted agricultural production (Ortloff and Kolata 1993). A recent high-resolution stalagmite record from central-eastern Brazil further revealed a general anti-phased relationship between the ASM and SASM during Bond events in the Holocene, similar to the general anti-phase relationship on longer timescales (Stríkis et al. 2011; Cheng et al. 2012b) (Fig. 9).

High-resolution and precise-dated speleothem records are required to reconstruct decadal-scale paleomonsoon variations. Such records are relatively few, in part because of the notion that on this timescale, the amplitude of monsoon related $\delta^{18}O$ change in the speleothem is
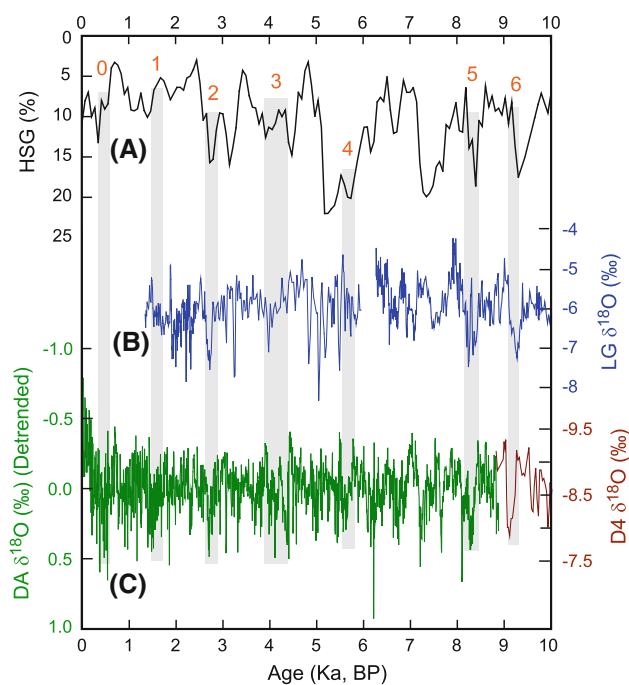
Fig. 9 Comparison of Bond events among the North Atlantic, ASM and SASM records (adapted from Stríkis et al. 2011). **a** Hematite stained quartz grain (HSG) record from the North Atlantic deep sea core VM 29-191 (Bond et al. 1997). **b** The SASM record from Lapa Grande Cave in central-eastern Brazil (Stríkis et al. 2011). **c** The ASM $\delta^{18}O$ record from two stalagmites DA (*green*, detrended) and D4 (*brown*) from Dongge Cave in southeastern China (Wang et al. 2005; Dykoski et al. 2005). The bond events 0–6 are indicated by the *grey bars*

expected to be small and sometimes indiscernible from the 'noise' produced from karst and non-climate related processes. Notwithstanding, high-resolution speleothem $\delta^{18}O$ records from Dandak and Jhumar Caves in central India (Sinha et al. 2011) and Wanxiang Cave in China bear remarkable similarity during the late Holocene (Berkelhammer et al. 2010). Records from both regions contain evidence for decadal-multidecadal length intervals of sustained reductions in monsoon rainfall (megadrought) during the last millennium. These megadroughts have been linked to discrete intervals of cooler conditions in the extratropical northern latitudes and southward displacement of the ITCZ (Sinha et al. 2011).

5 Equatorial-tropical records and possible links to the Walker circulation

While the ASM and SASM variations inferred from speleothem $\delta^{18}O$ records clearly describe the anti-phased ~23 ka precessional cycles, speleothem $\delta^{18}O$ records from sites near the equatorial-tropics (low latitudes (<10°)) tend to exhibit complex precipitation behavior at precessional bands with
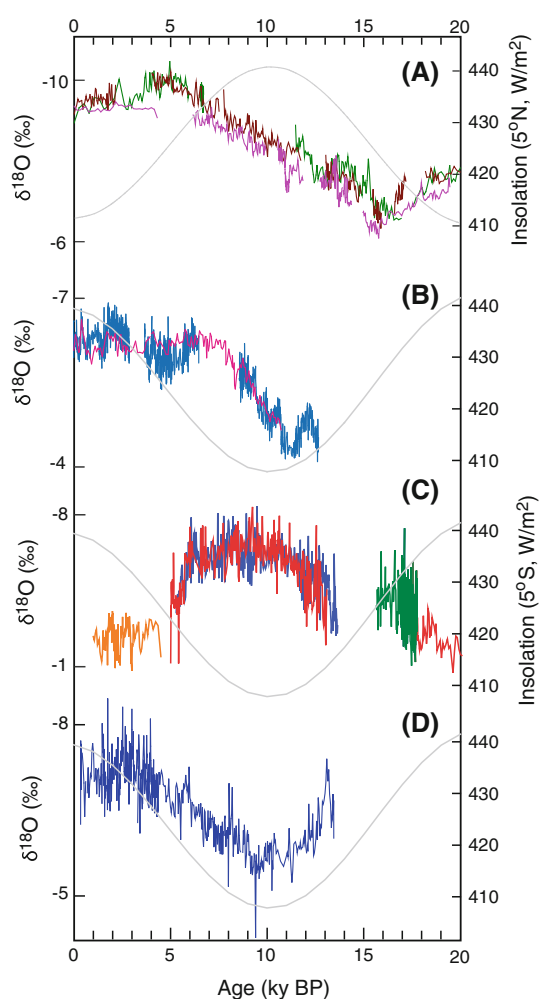
Fig. 10 Cave $\delta^{18}O$ records from equatorial-tropical areas. **a** The Borneo $\delta^{18}O$ record (~4°N, Malaysia, Partin et al. 2007). **b** The Liang Luar record (~8.5°S, Indonesia, Griffiths et al. 2009). **c** The cave $\delta^{18}O$ record from northeastern Brazil (~5.5°S, Cruz et al. 2009a). **d** The Cueva del Tigre Perdido record (~6°S, Peru, van Breukelen et al. 2008). *Different colors* denote different stalagmites. Summer insolation (*grey curves*) at 5°N (**a**) and 5°S (**b–d**) were plotted for comparison (Berger 1978)

some of their $\delta^{18}O$ changes tracking neither insolation nor $\delta^{18}O$ changes from other low latitude sites within the same hemisphere. For example, speleothem $\delta^{18}O$ variations spanning the last precession cycle from Liang Luar Cave in western Flores, Indonesia (~8.5°S, Griffiths et al. 2009), Borneo caves, Malaysia (~4°N, Partin et al. 2007), Cueva del Tigre Perdido Cave, northern Peru (~6°S, van Breukelen et al. 2008), and northeastern Brazil (~5.5°S, Cruz et al. 2009a) are quite different. While the $\delta^{18}O$ orbital-scale changes in the above two Asian records bear some similarities, even though they are located in two hemispheres respectively, the two South American records within the same hemisphere are nearly anti-phased (Figs. 1 and 10). These disparities may have resulted from complex changes in the Walker circulation

associated with deep monsoon convection over equatorial-tropical regions, perhaps tied to insolation and/or glacial boundary conditions (Clement et al. 2004; Cruz et al. 2009a). These complex phase relationships are, to some extent, expected, considering the dramatic changes observed in the zonal atmospheric circulations along the equatorial-tropics and associated large precipitation and temperature fluctuations between El Niño and La Niña years. Further investigations, particularly on longer timescales, are important to reach a comprehensive understanding about patterns of the paleoclimat change in the equatorial-tropical region and the possible cause of it.

6 Discussions

6.1 Orbital-scale variability

The speleothem $\delta^{18}O$ records indicate that long-term histories of the ASM and SASM are dominated by precessional cyclicity (e.g., Wang et al. 2008; Cheng et al. 2009b; van Breukelen et al. 2008; Cruz et al. 2005, 2007, 2009b; Wang et al. 2007a), suggesting a dominating role of summer insolation forcing. This mechanism agrees well with a series of simulation studies which indicate that increased summer solar radiation appears to be most effective in strengthening monsoons (e.g., Prell and Kutzbach 1987, 1992; Masson et al. 2000; Kutzbach et al. 2008; Yin and Berger 2011; Battisti et al. 2012). In contrast, marine proxy records from the Arabian Sea suggest a significant time lag (~ 8 ka) of the ISM in response to NHSI change on the precessional cycle (e.g., Clemens et al. 1991, 2010; Clemens and Prell 2003; Caley et al. 2011b). The ~ 8 ka phase lag has been linked to mechanisms of latent heat transport from the southern Indian Ocean and global ice volume influence on the ASM that lags NHSI by ~ 11 and 5 ka at precession bands, respectively (Clemens et al. 2010).

The apparent lag of the ISM, as inferred from the marine records, has recently been used to reinterpret Chinese speleothem $\delta^{18}O$ records, because a major portion of summer monsoon precipitation in southeastern China is presumed to result from the ISM system (Clemens et al. 2010). This interpretation singles out three distinctive components relevant to precipitation seasonality in southeastern China: summer (JJA, 48 % of total annual precipitation with $\delta^{18}O$ of ~ -8.78 ‰ originating from the Indian Ocean source), winter (SONDJFM, 34 % of total annual precipitation with $\delta^{18}O$ of ~ -6.60 ‰ from continental sources) and spring (AM, 18 % of total annual precipitation with $\delta^{18}O$ of ~ -3.14 ‰ from the Pacific source). The summer $\delta^{18}O$ signal in Chinese speleothem records (emanating from the ISM domain) has been deemed to exhibit a ~ 8 ka lag to NH June insolation. On the other hand, the residual $\delta^{18}O$ signal (non-summer precipitation) has been argued to stem from winter temperature influence and is in phase with the NH June (summer solstice) insolation change at precession bands. In this sense, the Chinese speleothem records reflect a mixed signal produced by aforementioned three components, yielding an orbital phase that lags mid-June insolation by ~ 2.9 ka.

If the EASM $\delta^{18}O$ records could be solely explained by mixing two distinct precipitation components, summer and non-summer, that have ~ 8 and 0 ka phase differences at precession bands respectively, it would be logical to presume that the $\delta^{18}O$ records may vary accordingly from ~ 8 ka lag (100 % summer precipitation) to in-phase (100 % non-summer precipitation) relative to NHSI change on precessional cycles, depending on the ratio of local summer/non-summer precipitations. In other words, this interpretation indeed predicts possible phase differences on precessional scale among speleothem $\delta^{18}O$ records in ASM regions, simply because seasonal distributions of precipitation and their moisture sources diverge significantly in the vast ASM domain. For instance, in eastern China, the summer monsoon onset is two months earlier in the south (in May) than in the north (in July). Furthermore, in southwestern China (e.g., Xiaobailong Cave, Yunnan (Fig. 1)), the spring Pacific moisture source is effectively absent, and thus the cave $\delta^{18}O$ records from this region should be theoretically different from the records in eastern China. However, thus far, neither the Xiaobailong record (Cai et al. 2006, 2011), nor any other published or unpublished Chinese cave records denote any resolvable phase differences at precession bands.

A recent speleothem $\delta^{18}O$ record from Tianmen Cave in the south-central Tibetan Plateau, located at considerable distance from southeastern China (Fig. 1), characterizes an ISM precipitation history over much of MIS 5 (Fig. 5) (Cai et al. 2010). The mean annual precipitation at this site is ~ 300 mm and ~ 86 % of it falls during summer months (June–September) when the ISM prevails in the area. The precipitation at this cave site virtually contains no moisture from the Pacific source and the winter precipitation component is also small and, therefore, this record is suitable for testing the orbital phase of the ISM. The Tianmen record is basically similar in both structure and timing to the cave records from southeastern China, suggesting no notable phase difference between Tianmen area and southeastern China (Fig. 5). In addition, two other cave records from the ISM region, the Timta record, northwestern India (~ 80 % of total annual precipitation from the ISM) and Qunf record, Oman (90 % of total annual precipitation from the ISM) (Fig. 1), also display a pattern during the past 15 ka which is essentially similar to those established from southeastern China (Fig. 4), even though modern precipitation patterns in the two cave sites are

rather different from those in southeastern China (Sinha et al. 2005; Fleitmann et al. 2003).

The comparison between speleothem records from ISM and EASM domains provides critical evidences that patterns of the cave $\delta^{18}O$ change in the vast ASM region are mostly coherent and their precession cyclicity appears to be in-phase with NHSI, notwithstanding substantial variance in local seasonal precipitation patterns and moisture sources. This observation suggests that the winter and summer monsoons may conceivably be in-phase at precession bands and, as a result, the overall phases are virtually similar over the vast ASM region regardless of the difference in seasonal precipitation distribution among different cave locations. A supporting line of evidence comes from the ice core $\delta^{18}O$ record of atmosphere O_2 ($\delta^{18}O_{atm}$). The Antarctic Vostok ice core $\delta^{18}O_{atm}$ record on an independent N_2/O_2 chronology (Suwa and Bender 2008) proves a striking similarity and strictly in-phase correlation with the EASM $\delta^{18}O$ record (Wang et al. 2008; Cheng et al. 2009b) on precessional cyclicity (Fig. 6). Severinghaus et al. (2009) further demonstrated a definite and precise correlation between the Dongge-Hulu $\delta^{18}O$ and high-resolution Siple Dome $\delta^{18}O_{atm}$ records on orbital-millennial timescale. This correlation reveals an important impact of monsoon rainfall on the biosphere process which amends the "Dole Effect". Moreover, because the ice core $\delta^{18}O_{atm}$ changes pertain to be an integrated global signal, very likely linked to tropical-subtropical hydrological variations (e.g., Severinghaus et al. 2009), their in-phase correlation with the EASM $\delta^{18}O$ record is consistent with the view that EASM variations are basically synchronous with those in the ISM and NASM domains, and incoherent with the idea that the EASM $\delta^{18}O$ record from southeastern China has a random orbital phase shaped primarily by local seasonal precipitation distribution. Nevertheless, the disparity between the marine records from the Arabian Sea and the ASM speleothem records remain an important question. Various possibilities can be raised such as whether the Arabian Sea domain has unique precipitation variability which is dissimilar to the ASM in Indian subcontinent and East Asia (e.g., Conroy and Overpeck 2011); or whether the ISM, including the Arabian Sea region, is different from the East Asian Monsoon, in response to insolation change (Yin et al. 2009). And finally, whether the marine ISM records primarily reflect changes in monsoon wind strength (monsoonal upwelling offshore the Arabian coast) or monsoon precipitation (Ruddiman 2006)? The ongoing work on long and continuous speleothem records from typical ISM regions (Gayatri Kathayat and Sebastian Breitenbach, personal communications) is particularly critical for further testing the aforementioned phasing issue.

One of the notable features of ASM and SASM speleothem records is the absence of significant 100-ka cycle.

Although some strong summer monsoon periods under glacial conditions were revealed from the Chinese Loess Plateau (Rousseau et al. 2009) which possibly occurred in the NASM domain as well (Mélières et al. 1997) (Fig. 6), the ASM reconstruction based on loess records from the Chinese Loess Plateau shows a strong 100-ka cycle, with strong (weak) summer monsoon occurring during interglacial (glacial) periods (e.g., Ding et al. 1995; Guo et al. 2011). The presence of dominant precessional cycles in Chinese speleothem records suggests a generally weak ice volume impact in tropical-subtropical monsoon regimes, and this appears to be consistent with a mechanism of ice volume threshold proposed in detail in Yin et al. (2009). We additionally offer here another possibility of threshold mechanism. If the speleothem $\delta^{18}O$ variations are largely dependent on the ratio of summer versus winter precipitation, each with its characteristic $\delta^{18}O$ values, rather than on absolute rainfall, a large increase in summer rainfall above certain threshold value could just result in a similar $\delta^{18}O$ value virtually determined by the $\delta^{18}O$ value of the summer monsoon component. In other words, once the summer monsoon dominates annual precipitations, speleothem $\delta^{18}O$ value does not drop further although summer rainfall might continue to increase. The EASM speleothem records are indeed characterized by comparable absolute $\delta^{18}O$ minima that coincide with NHSI peaks both during the glacial and interglacial periods (Fig. 6). At face value, this observation implies no significant weakening of the EASM at high summer insolation phases even during the full glacial periods in tropical-subtropical regions. On the other hand, speleothem growth in Yemen and Oman-locations that are at the current fringes of the ISM, occurred only during NHSI peaks in interglacial periods (Burns et al. 2001; Fleitmann et al. 2011), implying that the ISM was significantly weaker during glacial periods. The threshold hypothesis may explain this discrepancy, as the similar $\delta^{18}O$ values in the EASM record reached at the insolation peaks during both glacial and interglacial periods could result from a same threshold value, likely the $\delta^{18}O$ value of summer moisture component, which limits further decreases in cave $\delta^{18}O$ value after the EASM dominants annual precipitations. This mechanism thus implies that the actual monsoon intensity at insolation peak in glacial periods could be weaker than that in interglacial periods and thus reconcilable at least partially with Chinese loess records and cave records from the Arabian Peninsula. Nevertheless, this hypothesis requires a further test and multiple-proxy records from both ISM and EASM regions are especially valuable for the purpose.

6.2 Millennial-scale variability

ASM $\delta^{18}O$ records contain prominent millennial-length events that exhibit negative correlations with the $\delta^{18}O$

records from the SASM region. The observed anti-phased pattern between the ASM and SASM (Fig. 8) is consistent with the AMOC mechanism as mentioned previously.

Meteorological data over the last 50 years and simulations indicate a covariance between the SASM intensity and the SST in the neighboring southern tropical Atlantic (Barros et al. 2000; Liebmann et al. 2004; Vuille and Werner 2005). On millennial and even orbital timescales, the SST anomaly may also likely influence the SASM activity and associated rainfall in southern South America. During the last glacial period, for instance, millennial-scale changes in ocean heat circulation related to the bipolar see-saw mechanism may have changed meridional Atlantic SST gradients (Broecker 1998). Modeling efforts show that the weak ocean circulation may cause a positive SST anomaly in the South Atlantic (e.g., Crowley 1992), consistent with the result from ocean sediment cores off the Brazilian coast (e.g., Arz et al. 1998). A warm SST anomaly may in turn stimulate a persistent intense SASM and strong LLJ, which consequently supplies more isotopically depleted precipitation up to southern Brazil.

A recent oxygen isotope-enabled climate model simulation shows that isotope signatures of precipitation recorded in speleothems from eastern China during the H and/or YD events reflect reduced precipitation over the Indian subcontinent rather than a significant decrease over China (Pausata et al. 2011). The model simulates the reduced precipitation over India which produces isotopically enriched vapor transported eastwards into China. Consequently, increase in the $\delta^{18}O$ of Chinese cave carbonates associated with these events has been argued to reflect changes in the intensity of the ISM rather than the EASM (Pausata et al. 2011). As noted earlier in this paper, the EASM is rather a geographic notion- a monsoonal phenomenon that occurs in East Asia. Modern observations show that the ISM and EASM can be viewed as the up- and low- stream portion of the large ASM circulation system, respectively (Figs. 1 and 2) (e.g., Ding 2004; Ding et al. 2004). In this sense, the H and YD events in speleothem $\delta^{18}O$ records from southeastern China indicate a weakened ASM (Wang et al. 2001) (including the upstream ISM) (e.g., Yuan et al. 2004; Cheng et al. 2006) and thus, are reconcilable with the simulation result (Pausata et al. 2011). However, it is also noteworthy that other proxy records in eastern China indicate possible variances in precipitation associated with H and YD events (e.g., Zhou et al. 2001, 2005; Yancheva et al. 2007; Sun et al. 2010, 2011), in contrast with the simulation result that shows no precipitation changes in the region (Pausata et al. 2011).

6.3 Centennial-decadal-scale variability

A new speleothem record from central-eastern Brazil (Stríkis et al. 2011) revealed a series of strong monsoon events on centennial-decadal timescales during the Holocene that are correlated to Bond events recorded by marine sediments from the North Atlantic Ocean (Bond et al. 1997). These events are broadly anti-phase with weak ASM events (Wang et al. 2005; Fleitmann et al. 2007; Cheng et al. 2009a) (Fig. 9). Not unlike their millennial-scale counterparts, these abrupt events are primarily linked to anomalous cross-equatorial flow induced by negative AMOC phases and resulting SST positive anomalies in the southern tropical Atlantic (Barros et al. 2000; Liebmann et al. 2004), and this may have sequentially modulated not only the monsoon in South America (Stríkis et al. 2011) but also affected the ASM during the Holocene (Wang et al. 2005; Cheng et al. 2009a; Sinha et al. 2011). In fact, Bond events are correlated to solar radiation variations inferred from ^{14}C production and ^{10}Be flux changes (Bond et al. 2001). A set of high resolution and precisely dated speleothem records also show evidence for a possible connection between solar radiation and Holocene climate changes in the ISM (e.g., Neff et al. 2001; Fleitmann et al. 2003), EASM (Wang et al. 2005), SASM (Stríkis et al. 2011), and North American Monsoon (Asmerom et al. 2007). The variability of the solar radiation is however rather small in amplitude. Some amplify mechanisms must exist to trigger worldwide climate change and one of such mechanisms proposed by Emile-Geay et al. (2007) involves the SST and in turn ENSO as a mediator between the solar forcing and the resulting climate change.

7 Summary: the PM and GPM

Because it is yet difficult to extract detail paleo-seasonality information from proxy records, we consider the PM to describe alternation of a mean climatic condition between two (or more) states on various timescales (i.e., orbital, millennial, centennial, decadal and annual timescales). Although, mechanisms driving PM oscillations are quite distinct on different timescales, their alternation patterns and global scope, inferred from well-distributed speleothem records from both hemispheres, are indeed comparable to the modern annual monsoonal scenario. On orbital timescale, the ASM and SASM intensities have oscillated between strong (during high summer insolation times) and weak (during low summer insolation times) states, respectively. The anti-phased relationship between the ASM and SASM on orbital timescale (Fig. 6) demonstrates an important aspect of the GPM scenario with summer insolation as the major driving forcing. Orbital variations in

ASM and SASM intensities were punctuated by a series of millennial-length events at least over the past two glacial-interglacial periods. Such variations may again be viewed as an oscillation between two states on millennial timescale with weak ASM events correlating with strong SASM events and vice versa. This millennial-scale pattern of climate variability conforms remarkably well to climate model projections, particularly with respect to the temporal synchrony of hemispherically asymmetric response of the monsoon system that accompanied the large-scale temperature fluctuations documented in the Greenland ice cores (Wang et al. 2008). These events show the global extent and may be casually linked to AMOC changes and the associated shifts in the mean latitudinal location of the ITCZ, asymmetry in the Hadley circulation in two hemispheres and SST anomalies (e.g., Lindzen and Hou 1988; Wang et al. 2006, 2007a, b). On centennial to decadal timescales, variability in the ASM and SASM inferred from speleothem records also point to a PM pattern with some features that are similar to their millennial counterparts (e.g., Wang et al. 2005; Cheng et al. 2009a; Stríkis et al. 2011; Cheng et al. 2012b). In summary, speleothem records demonstrate a GPM phenomenon with three key features that are analogous to modern observations of the GM scenario: (1) Paleomonsoonal oscillations on different timescales (Orbital-millennial and possibly even on centennial-decadal); (2) their global extent; and (3) inter-hemispheric anti-phased relationship between the ASM and SASM domains.

References

Alley RB, Mayewski PA, Sowers T, Stuiver M, Taylor KC, Clark PU (1997) Holocene climatic instability: a prominent, widespread event 8200 yr ago. Geology 25:483–486

An ZS (2000) The history and variability of the East Asian palaeomonsoon climate. Quat Sci Rev 19:171–187

Arz HW, Pätzold J, Wefer G (1998) Correlated millennial-scale changes in surface hydrography and terrigenous sediment yield inferred from last glacial marine deposits off northeastern Brazil. Quat Res 50:157–166

Arz HW, Lamy F, Pätzold J, Muller PJ, Prins M (2003) Mediterranean moisture source for an early-Holocene humid period in the northern Red Sea. Science 300:118–121

Asmerom Y, Polyak V, Burns S, Rassmussen J (2007) Solar forcing of Holocene climate: new insights from a speleothem record, southwestern United States. Geology 35:1–4

Asmerom Y, Polyak VJ, Burns SJ (2010) Variable winter moisture in the southwestern United States linked to rapid glacial climate shifts. Nat Geosci 3:114–117

Badertscher S, Fleitmann D, Cheng H, Edwards RL, Göktürk OM, Zumbühl A, Leuenberger M, Tüysüz O (2011) Pleistocene water intrusions from the Mediterranean and Caspian seas into the Black Sea. Nat Geosci 4:236–239

Bar-Matthews M, Ayalon A, Gilmour M, Matthews A, Hawkesworth CJ (2003) Sea-land oxygen isotopic relationships from planktonic foraminifera and speleothems in the Eastern Mediterranean region and their implication for paleorainfall during interglacial intervals. Geochimt Cosmochim Acta 67:3181–3199

Barros V, Gonzalez M, Liebmann B, Camilloni I (2000) Influence of the South Atlantic convergence zone and South Atlantic sea surface temperature on interannual summer rainfall variability in southeastern South America. Theor Appl Climatol 67:123–133

Battisti D, Ding QH, Roe G (2012) The relative importance of orbital and glacial boundary conditions on the climate and isotopic composition of precipitation (to be submitted)

Berger AL (1978) Long-term variations of caloric insolation resulting from the Earth's orbital elements. Quat Res 9:139–167

Berkelhammer M, Sinha A, Mudelsee M, Cannariato KG (2010) Persistent multidecadal power in the Indian Summer Monsoon. Earth Planet Sci Lett 290:166–172. doi:10.1016/j.epsl.2009.12.017

Bond G, Showers W, Cheseby M, Lotti R, Almasi P, deMenocal P, Priore P, Cullen H, Hajdas I, Bonani G (1997) A pervasive millennial-scale cycle in North Atlantic Holocene and Glacial climates. Science 278:1257–1266

Bond G, Kromer B, Beer J, Muscheler R, Evans MN, Showers W, Hoffmann S, Lotti-Bond R, Hajdas I, Bonani G (2001) Persistent solar influence on North Atlantic climate during the Holocene. Science 294:2130–2136

Broecker WS (1998) Paleocean circulation during the last deglaciation: a bipolar seesaw? Paleoceanography 13:119–121

Burns SJ, Matter A, Frank N, Mangini A (1998) Speleothem-based paleoclimate record from northern Oman. Geology 26:499–502

Burns SJ, Fleitmann D, Matter A, Neff U, Mangini A (2001) Speleothem evidence from Oman for continental pluvial events during interglacial periods. Geology 29:623–626

Burns SJ, Fleitmann D, Matter A, Kramers J, Al-Subbary A (2003) Indian Ocean climate and an absolute chronology over Dansgaard/Oeschger events 9–13. Science 301:1365–1367

Cai YJ, An ZS, Cheng H, Edwards RL, Kelly MJ, Liu WG, Wang XF, Shen CC (2006) High-resolution absolute-dated Indian Monsoon record between 53 and 36 ka from Xiaobailong Cave, southwestern China. Geology 34:621–624

Cai YJ, Cheng H, An ZS, Edwards RL, Wang XF, Tan LC, Wang J (2010) Oxygen isotope records of precipitation from the south-central Tibetan Plateau during the last interglaciation: clues from speleothems. Geology 38:243–246

Cai YJ, Tan LC, Cheng H, An ZS, Edwards RL, Shen CC (2011) The variation of the Indian Monsoon over the past 245 kyr: speleothem records from Xiaobailong Cave, southwest China. XVIII. INQUA meeting abstract. 2011 in Bern, Switzerland

Caley T, Malaizé B, Revel M, Ducassou E, Wainer K, Ibrahim M, Shoeaib D, Migeon S, Marieu V (2011a) Orbital timing of the Indian, East Asian and African boreal monsoons and the concept of a 'global monsoon'. Quat Sci Rev 30:3705–3715

Caley T, Malaizé B, Zaragosi S, Rossignol L, Bourget J, Eynaud F, Martinez P, Giraudeau J, Charlier K, Ellouz-Zimmermann N (2011b) New Arabian Sea records help decipher orbital timing of Indo-Asian monsoon. Earth Planet Sci Lett 308:433–444

Cheng H, Edwards RL, Wang YJ, Kong XG, Ming YF, Gallup CD, Kelly MJ, Wang XF, Liu WG (2006) A penultimate glacial monsoon record from Hulu Cave and two-phase glacial terminations. Geology 34:217–220

Cheng H, Fleitmann D, Edwards RL, Wang XF, Cruz FW, Auler AS, Mangini A, Wang YJ, Kong XG, Burns SJ, Matter A (2009a)

Timing and structure of the 8.2 kyr B.P. event inferred from $\delta^{18}O$ records of stalagmites from China, Oman, and Brazil. Geology 37:1007–1010

Cheng H, Edwards RL, Broecker WS, Denton GH, Kong XG, Wang YJ, Zhang R, Wang XF (2009b) Ice age terminations. Science 326:248–252

Cheng H, Edwards RL, Haug GH (2010) Comment on "On linking climate to Chinese dynastic change: Spatial and temporal variations of monsoonal rain". Chinese Sci Bull 55:3734–3737

Cheng H, Zhang PZ, Spötl C, Edwards RL, Cai YJ, Zhang DZ, Sang WC, Tan M, An ZS (2012a) The climatic cyclicity in semiarid-arid central Asia over the past 500,000 years. Geophys Res Lett 39:L01705. doi:10.1029/2011GL050202

Cheng H, Sinha A, Colman SM (2012b) Monsoon climate—will summer rain increase or decrease in monsoon regions? (Past). PAGES Newsletter 20:27

Chiang JCH, Bitz CM (2005) Influence of high latitude ice cover on the marine intertropical convergence zone. Clim Dyn 25:477–496

Chiang JCH, Biasutti M, Battisti DS (2003) Sensitivity of the Atlantic intertropical convergence zone to last glacial maximum boundary conditions. Paleoceanography 18:1094. doi:10.1029/2003PA000916

Clemens SC, Prell WL (2003) A 350,000 year summer-monsoon multi-proxy stack from the Owen Ridge, Northern Arabian Sea. Mar Geol 201:35–51

Clemens SC, Prell WL, Murray D, Shimmield G, Weedon D (1991) Forcing mechanisms of the Indian Ocean monsoon. Nature 353:720–725

Clemens SC, Prell WL, Sun YB (2010) Orbital-scale timing and mechanisms driving Late Pleistocene Indo-Asian summer monsoons: reinterpreting cave speleothem $\delta^{18}O$. Paleoceanograpgy 25:PA4207. doi:10.1029/2010PA001926

Clement AC, Peterson LC (2008) Mechanisms of abrupt climate change of the last glacial period. Rev Geophys 46:RG4002. doi:10.1029/2006RG000204

Clement AC, Hall A, Broccoli AJ (2004) The importance of precessional signals in the tropical climate. Clim Dyn 22:327–341

Conroy JL, Overpeck JT (2011) Regionalization of present-day precipitation in the greater monsoon region of Asia. J Clim. doi:10.1175/2011JCLI4033.1

Crombie MK, Arvidson RE, Sturchio NC, El Alfy Z, Zeid KA (1997) Age and isotopic constraints on Pleistocene pluvial episodes in the western desert, Egypt. Palaeogeogr Palaeoclimatol Palaeoecol 130:337–355

Crowley TJ (1992) North Atlantic deep water cools the southern hemisphere. Paleoceanography 7:489–499

Cruz FW, Burns SJ, Karmann I, Sharp WD, Vuille M, Cardoso AO, Ferrari JA, Dias PLS, Viana O Jr (2005) Insolation-driven changes in atmospheric circulation over the past 116,000 years in subtropical Brazil. Nature 434:63–66

Cruz FW, Burns SJ, Karmann I, Sharp WD, Vuille M (2006) Reconstruction of regional atmosphere circulation features during the late Pleistocene in subtropical Brazil from oxygen isotope composition of speleothems. Earth Planet Sci Lett 248:494–506

Cruz FW, Burns SJ, Jercinovic M, Karmann I, Sharp WD, Vuille M (2007) Evidence of rainfall variations in southern Brazil from trace element ratios (Mg/Ca and Sr/Ca) in a late pleistocene stalagmite. Geochim Cosmochim Acta 71:2250–2263

Cruz FW, Vuille M, Burns SJ, Wang XF, Cheng H, Werner M, Edwards RL, Karmann I (2009a) Orbitally driven east-west antiphasing of South American precipitation. Nat Geosci 2:210–214

Cruz FW, Wang XF, Auler A, Vuille M, Burns SJ, Edwards RL, Karmann I, Cheng H (2009b) Orbital and millennial-scale precipitation changes in Brazil from speleothem records. Dev Paleoenvironmental Res 14:29–60

Dayem KE, Molnar P, Battisti DS, Roe GH (2010) Lessons learned from oxygen isotopes in modern precipitation applied to interpretation of speleothem records of paleoclimate from eastern Asia. Earth Planet Sci Lett 295:219–230

Ding YH (1992) Summer monsoon rainfalls in China. J Meteor Soc Jpn 70:373–396

Ding YH (2004) Seasonal march of East Asian monsoon. In: Chang CP (ed) East Asian monsoon. World Scientific, Singapore, p 560

Ding ZL, Liu TS, Rutter NW, Yu ZW, Guo ZT, Zhu RX (1995) Ice-volume forcing of the East Asia winter monsoon variations in the past 800,000 years. Quat Res 44:149–159

Ding YH, Li CY, Liu YJ (2004) Overview of the South China Sea monsoon experiment. Adv Atmospheric Sci 21:343–360

Drysdale RN, Hellstrom JC, Zanchetta G, Fallick AE, Sánchez Goñi MF, Couchoud I, McDonald J, Maas R, Lohmann G, Isola I (2009) Evidence for obliquity forcing of glacial termination II. Science 325:1527–1531

Dykoski CA, Edwards RL, Cheng H, Yuan DX, Cai YJ, Zhang ML, Lin YS, Qing JM, An ZS, Revenaugh J (2005) A high-resolution, absolute-dated Holocene and deglacial Asian monsoon record from Dongge Cave, China. Earth Planet Sci Lett 233:71–86

Emile-Geay J, Cane MA, Seager R, Kaplan A, Almasi P (2007) El Niño as a mediator of the solar influence on climate. Paleoceanography 22:PA3210. doi:10.1029/2006PA001304

Fleitmann D, Burns SJ, Mudelsee M, Neff U, Kramers J, Mangini A, Matter A (2003) Holocene forcing of the Indian monsoon recorded in a stalagmite from Southern Oman. Science 300:1737–1739

Fleitmann D, Burns SJ, Mangini A, Mudelsee M, Kramers J, Villa I, Neff U, Al-Subbary AA, Buettner A, Hippler D, Matter A (2007) Holocene ITCZ and Indian monsoon dynamics recorded in stalagmites from Oman and Yemen (Socotra). Quat Sci Rev 26:170–188

Fleitmann D, Burns SJ, Pekala M, Mangini A, Al-Subbary A, Al-Aowah M, Kramers J, Matter A (2011) Holocene and Pleistocene pluvial periods in Yemen, southern Arabia. Quat Sci Rev 30:783–787

Fontugne M, Calvert SE (1992) Late Pleistocene variability of the carbon isotopic composition of organic matter in the Eastern Mediterranean: Monitor of changes in carbon sources and atmosphere CO_2 concentrations. Paleoceanography 7:1–20

Göktürk OM, Fleitmann D, Badertscher S, Cheng H, Edwards RL, Leuenberger M, Fankhauser A, Tüysüz O, Kramers J (2011) Climate on the southern Black Sea coast during the Holocene: Implications from the Sofular Cave record. Quat Sci Rev 30:2433–2445

Griffiths ML, Drsydale RN, Gagan MK, Zhao JX, Ayliffe LK, Hellstrom JC, Hantoro WS, Frisia S, Feng YX, Cartwright I, St Pierre E, Fischer MJ, Suwargadi BW (2009) Increasing Australian–Indonesian monsoon rainfall linked to early Holocene sea-level rise. Nat Geosci 2:636–639

Guo ZT, Zhou X, Wu HB (2011) Glacial-interglacial water cycle, global monsoon and atmospheric methane changes. Clim Dyn. doi:10.1007/s00382-011-1147-5

Hoffmann G (2003) Taking the pulse of the tropical water cycle. Science 301:776–777

Johnson KR, Ingram BL (2004) Spatial and temporal variability in the stable isotope systematics of modern precipitation in China: implications for paleoclimate reconstructions. Earth Planet Sci Lett 220:365–377

Kanner LC, Burns SJ, Cheng H, Edwards RL (2012) High latitude forcing of the South American summer monsoon during the last glacial. Science 335:570–573

Kelly MJ, Edwards RL, Cheng H, Yuan DX, Cai Y, Zhang ML, Lin YS, An ZS (2006) High resolution characterization of the Asian monsoon between 146,000 and 99,000 years B.P. from Dongge Cave, China. Paleogeogr Paleoclimatol Paleoecol 236:20–38

Kutzbach JE (1981) Monsoon climate of the early Holocene: climate experiment with the Earth's orbital parameters for 9000 years ago. Science 214:59–61

Kutzbach JE, Liu XD, Liu ZY, Chen GS (2008) Simulation of the evolutionary response of global summer monsoons to orbital forcing over the last 280,000 years. Clim Dyn 30:567–579

Lachniet MS (2009) Climatic and environmental controls on speleothem oxygen-isotope values. Quat Sci Rev 28:412–432

Lee J-E, Johnson K, Fung I (2009) Precipitation over South America during the last glacial maximum: an analysis of the "amount effect" with a water isotope-enabled general circulation model. Geophys Res Lett 36:L19701. doi:10.1029/2009GL039265

LeGrande AN, Schmidt GA (2009) Sources of Holocene variability of oxygen isotopes in paleoclimate archives. Clim Past 5:441–455

Levermann A, Schewe J, Petoukhov V, Held H (2009) Basic mechanism for abrupt monsoon transitions. Proc Nat Acad Sci 106:20572–20577

Liebmann B, Vera CS, Carvalho LMV, Camilloni IA, Hoerling MP, Allured D, Barros VR, Báez J, Bidegain M (2004) An observed trend in Central South American precipitation. J Clim 17:4357–4367

Lindzen RS, Hou AY (1988) Hadley circulations for zonally averaged heating centered off the equator. J Atmos Sci 45:2416–2427

Lisiecki L, Raymo MA (2005) Plio-Pleistocene stack of 57 globally distributed benthic δ^{18}O records. Paleoceanography 20:522–533

Ma ZB, Cheng H, Tan M, Edwards RL, Li HC, Duan WH, Wang X, Kelly M (2012) The timing and structure of the Younger Dryas event in northern China. Quat Sci Rev 41:83–93

Maher BA (2008) Holocene variability of the East Asian summer monsoon from Chinese cave records: a reassessment. Holocene 18:861–866

Masson V, Braconnot P, Jouzel J, de Nobler N (2000) Simulation of intense monsoons under glacial conditions. Geophys Res Lett 27:1747–1750

Neff U, Burns SJ, Mangini A, Mudelsee M, Fleitmann D, Matter A (2001) Strong coherence between solar variability and the monsoon in Oman between 9 and 6 ka ago. Nature 411:290–293

Fairchild IJ, Smith CL, Baker A, Fuller L, Spötl C, Mattey D, McDermott F, EIMF (2006) Modification and preservation of environmental signals in speleothems. Earth Sci Rev 75:105–153

McIntyre A, Ruddiman WF, Karlin K, Mix AC (1989) Surface water response of the equatorial Atlantic Ocean to orbital forcing. Paleoceanography 4:19–55

Mélières MA, Rossignol-Strick R, Malaizé B (1997) Relation between low-latitude insolation and δ^{18}O change of atmospheric oxygen for the last 200 kyrs, as revealed by Mediterranean sapropels. Geophys Res Lett 24:1235–1238

Ortloff CR, Kolata AL (1993) Climate and collapse-agro-ecological perspectives on the decline of the Tiwanaku state. J Arch Sci 20:195–221

Partin JW, Cobb KM, Adkins JF, Clark B, Fernandez DP (2007) Millennial-scale trends in west Pacific warm pool hydrology since the last glacial maximum. Nature 449:452–455

Partridge TC, deMenocal PB, Lorentz SA, Paiker MJ, Vogel JC (1997) Orbital forcing of climate over South Africa: a 200,000-year rainfall record from the Pretoria Saltpan. Quat Sci Rev 16:1125–1133

Pausata FSR, Battisti DS, Nisancioglu KH, Bitz CM (2011) Chinese stalagmite δ^{18}O controlled by changes in the Indian monsoon during a simulated Heinrich event. Nat Geosci 4:474–480

Pokras EM, Mix AC (1987) Earth's precession cycle and quaternary climatic change in tropical Africa. Nature 326:486–487

Prell WL, Kutzbach JE (1987) Monsoon variability over the past 150,000 years. J Geophys Res 92:8411–8425

Prell WL, Kutzbach JE (1992) Sensitivity of the Indian monsoon to forcing parameters and implications for its evolution. Nature 360:647–652

Qian W, Deng Y, Zhu Y, Dong W (2002) Demarcating the worldwide monsoon. Theor Appl Climatol 71:1–16

Reuter J, Stott L, Sinha A, Cheng H, Edwards RL (2009) A new perspective on the hydroclimate variability in Northern South America during the little ice age. Geophys Res Lett 36:L21706. doi:10.1029/2009GL041051

Rohling EJ, Abu-Zied R, Casford JLS, Hayes A, Hoogakker BAA (2009) The marine environment: present and past. In: Woodward JC (ed) The physical geography of the Mediterranean. Oxford University Press, Oxford, UK, pp 33–67

Rossignol-Strick M (1983) African monsoons, an immediate climate response to orbital insolation. Nature 304:46–49

Rossignol-Strick M, Nesteroff W, Olive P, Vergnaud-Grazzini C (1982) After the deluge: mediterranean stagnation and sapropel formation. Nature 295:105–110

Rousseau DD, Wu N, Pei Y, Li F (2009) Three exceptionally strong East-Asian summer monsoon events during glacial times in the past 470 kyr. Clim Past 5:157–169

Ruddiman WF (2006) What is the timing of orbital-scale monsoon changes? Quat Sci Rev 25:657–658

Ruddiman WF (2008) Earth's climate: past and future. W H Freeman & Co, New York

Schewe J, Levermann A, Cheng H (2011) A critical humidity threshold for monsoon transitions. Clim Past Dis 7:1737–1765

Severinghaus JP, Beaudette R, Headly MA, Taylor K, Brook EJ (2009) Oxygen-18 of O_2 records the impact of abrupt climate change on the terrestrial biosphere. Science 324:1431–1434

Shakun JD, Burns SJ, Fleitmann D, Kramers J, Matter A, Ai-Subary A (2007) A high-resolution, absolute-dated deglacial speleothem record of Indian Ocean climate from Socotra Island, Yemen. Earth Planet Sci Latt 259:442–456

Sinha A, Cannariato KG, Stott LD, Li HC, You CF, Cheng H, Edwards RL, Singh IB (2005) Variability of southwest Indian summer monsoon precipitation during the Bølling–Allerød. Geology 33:813–816

Sinha A, Stott LD, Berkelhammer M, Cheng H, Edwards RL, Aldenderfer M, Mudelsee M, Buckley B (2011) A global context for monsoon megadroughts during the past millennium. Quat Sci Rev 30:47–62

Stríkis NM, Cruz FW, Cheng H, Karmann I, Edwards RL, Vuille M, Wang XF, de Paula MS, Novello VF, Auler AS (2011) Abrupt variations in South American monsoon rainfall during the Holocene based on a speleothem record from central-eastern Brazil. Geology 39:1075–1078

Sun YB, Wang XL, Liu QS, Clemens SC (2010) Impacts of post-depositional processes on rapid monsoon signals recorded by the last glacial loess deposits of northern China. Earth Planet Sci Lett 289:171–179

Sun YB, Clemens SC, Morrill C, Lin XP, Wang XL, An ZS (2011) Influence of Atlantic meridional overturning circulation on the East Asian winter monsoon. Nature Geosci 5:46–49

Suwa M, Bender ML (2008) Chronology of the Vostok ice core constrained by O2/N2 ratios of occluded air, and its implication for the Vostok climate records. Quat Sci Rev 27:1093–1106

Svensson A, Andersen KK, Bigler M, Clausen HB, Dahl-Jensen D, Davies SM, Johnsen SJ, Muscheler R, Parrenin F, Rasmussen SO, Röthlisberger R, Seierstad I, Steffensen JP, Vinther BM (2008) A 60,000 year Greenland stratigraphic ice core chronology. Clim Past 4:47–57

Szabo BJ, Haynes JCV, Maxwell TA (1995) Ages of quaternary pluvial episodes determined by uranium-series and radiocarbon

dating of lacustrine deposits of Eastern Sahara. Palaeogeogr Palaeoclimatol Palaeoecol 113:227–242

Trenberth KE, Stepaniak DP, Caron JM (2000) The global monsoon as seen through the divergent atmospheric circulation. J Clim 13:3969–3993

Tzedakis PC (2007) Seven ambiguities in the Mediterranean palae-oenvironmental narrative. Quat Sci Rev 26:2042–2066

Vaks A, Bar-Matthews M, Ayalon A, Matthews A, Frumkin A, Dayan U, Halicz L, Almogi-Labin A, Schilman B (2006) Paleoclimate and location of the border between Mediterranean climate region and the Saharo-Arabian desert as revealed by speleothems from the northern Negev Desert, Israel. Earth Planet Sci Lett 249:384–399

Vaks A, Bar-Matthews M, Ayalon A, Matthews A, Halicz L, Frumkin A (2007) Desert speleothems reveal climatic window for African exodus of early modern humans. Geology 35:831–834

Vaks A, Bar-Matthews M, Matthews A, Ayalon A, Frumkin A (2010) Middle-late quaternary paleoclimate of northern margins of the Saharan-Arabian desert: reconstruction from speleothems of Negev Desert, Israel. Quat Sci Rev 29:2647–2662

van Breukelen MR, Vonhof HB, Hellstrom JC, Wester WCG, Kroon D (2008) Fossil dripwater in stalagmites reveals Holocene temperature and rainfall variation in Amazonia. Earth Planet Sci Lett 275:54–60

Vuille M, Werner M (2005) Stable isotopes in precipitation recording South American summer monsoon and ENSO variability: observations and model results. Clim Dyn 25:401–413

Wagner JDM, Cole JE, Beck JW, Patchett PJ, Henderson GM, Barnett HR (2010) Moisture variability in the southwestern United States linked to abrupt glacial climate change. Nat Geosci 3:110–113

Waldmann N, Torfstein A, Stein M (2010) Northward intrusions of low- and mid-latitude storms across the Saharo-Arabian belt during past interglacials. Geology 38:567–570

Wang PX (2009) Global monsoon in a geological perspective. Chinese Sci Bull 54:1113–1136

Wang B, Ding Q (2006) Changes in global monsoon precipitation over the past 56 years. Geophys Res Lett 33:L06711. doi:10.1029/2005GL025347

Wang B, Ding Q (2008) Global monsoon: dominant mode of annual variation in the tropics. Dyn Atmos Oceans 44:165–183. doi:10.1016/j.dynatmoce.2007.05.002

Wang YJ, Cheng H, Edwards RL, An ZS, Wu JY, Shen CC, Dorale JA (2001) A high-resolution absolute-dated late pleistocene monsoon record from Hulu Cave, China. Science 294:2345–2348

Wang XF, Auler AS, Edwards RL, Cheng H, Cristalli PS, Smart PL, Richards DA, Shen C–C (2004) Northeastern Brazil Wet periods linked to distant climate anomalies and rainforest boundary changes. Nature 432:740–743

Wang YJ, Cheng H, Edwards RL, He Y, Kong XG, An ZS, Wu JY, Kelly MJ, Dykoski CA, Li X (2005) The Holocene Asian monsoon: links to solar changes and North Atlantic climate. Science 308:854–857

Wang XF, Auler AS, Edwards RL, Cheng H, Ito E, Solheid M (2006) Interhemispheric anti-phasing of rainfall during the last glacial period. Quat Sic Rev 25:3391–3403

Wang XF, Auler AS, Edwards RL, Cheng H, Ito E, Solheid M, Wang YJ, Kong XG (2007a) Millennial-scale precipitation changes in southern Brazil over the past 90,000 years. Geophys Res Lett 34:L23701. doi:10.1029/2007GL031149

Wang XF, Edwards RL, Auler AS, Cheng H, Ito E (2007b) Millennial-scale interhemispheric asymmetry of low-latitude precipitation: speleothem evidences and possible high-latitude forcing. Am Geophys Union Monogr 173:279–294

Wang YJ, Cheng H, Edwards RL, Kong XG, Shao XH, Chen ST, Wu JY, Jiang X, Wang XF, An ZS (2008) Millennial-and orbital-scale changes in the East Asian monsoon over the past 224,000 years. Nature 451:1090–1093

Wang PX, Wang B, Kiefer T (2009) Global monsoon in observations, simulations and geological records. PAGES News 17:82–83

Weldeab S, Lea DW, Schneider RR, Andersen N (2007) 155,000 years of West African monsoon and ocean thermal evolution. Science 316:1303–1307

Yancheva G, Nowaczyk NR, Mingram J, Dulski P, Schettler G, Negendank JFW, Liu JQ, Sigman DM, Peterson LC, Haug GH (2007) Influence of the intertropical convergence zone on the East-Asian monsoon. Nature 445:74–77

Yin QZ, Berger A (2011) Individual contribution of insolation and CO2 to the interglacial climates of the past 800,000 years. Clim Dyn. doi:10.1007/s00382-011-1013-5

Yin QZ, Berger A, Crucifix M (2009) Individual and combined effects of ice sheets and precession on. MIS-13 climate. Clim Past 5:229–243

Yuan DX, Cheng H, Edwards RL, Dykoski CA, Kelly MJ, Zhang ML, Qin JM, Lin YS, Wang YJ, Wu JY, Dorale JA, An ZS, Cai YJ (2004) Timing, duration, and transitions of the last interglacial Asian monsoon. Science 304:575–578

Zhang R, Delworth TL (2005) Simulated tropical response to a substantial weakening of the Atlantic thermohaline circulation. J Clim 18:1853–1860

Zhang PZ, Cheng H, Edwards RL, Chen FH, Wang YJ, Yang XL, Liu J, Tan M, Wang XF, Liu JH, An CL, Dai ZB, Zhou J, Zhang DZ, Jia JH, Jin LY, Johnson KR (2008) A test of climate, sun, and culture relationships from a 1810-year Chinese Cave record. Science 322:940–942

Zhou JY, Lau K-M (1998) Does a monsoon climate exist over South America? J Clim 11:1020–1040

Zhou WJ, Head MJ, An ZS, Deckker PD, Liu ZY, Liu XD, Lu XF, Donahue D, Jull AJT, Beck JW (2001) Terrestrial evidence for a spatial structure of tropical-polar interconnections during the younger Dryas episode. Earth Planet Sci Lett 191:231–239

Zhou WJ, Xie SC, Meyers PA, Zheng YH (2005) Reconstruction of late glacial and Holocene climate evolution in southern China from geolipids and pollen in the Dingnan peat sequence. Org Geochem 36:1272–1284

Zhou TJ, Yu R, Li H, Wang B (2008) Ocean forcing to changes in global monsoon precipitation over the recent half century. J Clim 21:3833–3852

Ziegler M, Tuenter E, Lourens LJ (2010) The precession phase of the boreal summer monsoon as viewed from the eastern Mediterranean (ODP Site 968). Quat Sci Rev 29:1481–1490